Unveiling the mechanisms of carboxylic acid esterification on acid zeolites for biomass-to-energy: A review of the catalytic process through experimental and computational studies

Glaucio José Gomes, María Fernanda Zalazar, Janine Carvalho Padilha, Michelle Budke Costa, Claudio Leones Bazzi, Pedro Augusto Arroyo

PII: S0045-6535(23)03149-1

DOI: https://doi.org/10.1016/j.chemosphere.2023.140879

Reference: CHEM 140879

To appear in: *ECSN*

Received Date: 5 September 2023

Revised Date: 19 November 2023

Accepted Date: 1 December 2023

Please cite this article as: Gomes, Glaucio.José., Zalazar, Marí.Fernanda., Padilha, J.C., Costa, M.B., Bazzi, C.L., Arroyo, P.A., Unveiling the mechanisms of carboxylic acid esterification on acid zeolites for biomass-to-energy: A review of the catalytic process through experimental and computational studies, *Chemosphere* (2024), doi: https://doi.org/10.1016/j.chemosphere.2023.140879.

Unveiling the mechanisms of carboxylic acid esterification on acid zeolites for biomass-to-energy: A review of the catalytic process through experimental and computational studies

Glaucio José Gomes[1,2,4*], *María Fernanda Zalazar*[1]*, *Janine Carvalho Padilha*[4], *Michelle Budke Costa*[3], *Claudio Leones Bazzi*[3], *Pedro Augusto Arroyo*[2]

[1] Laboratorio de Estructura Molecular y Propiedades (LEMyP), Instituto de Química Básica y Aplicada del Nordeste Argentino, (IQUIBA-NEA), Consejo Nacional de Investigaciones Científicas y Técnicas, Universidad Nacional del Nordeste (CONICET-UNNE), Avenida Libertad 5460, 3400, Corrientes, Argentine.

[2] Laboratórios de Catálise Heterogênea e Biodiesel (LCHBio), Universidade Estadual de Maringá (UEM), Avenida Colombo, 5790, (87020-900), Maringá, Paraná, Brazil.

[3] Universidade Tecnológica Federal do Paraná (UTFPR), Avenida Brasil 4232, (85884-000) Medianeira, Brazil.

[4] Programa de Pós-Graduação Interdisciplinar em Energia e Sustentabilidade, Universidade Federal da Integração Latino-Americana (UNILA), Avenida Presidente Tancredo Neves, 3838, (85870-650), Foz do Iguaçu-Paraná, Brasil

* Corresponding authors.

Email addresses: mfzalazar@conicet.gov.ar (M .F. Zalazar), glauciojgomes@gmail.com (G. J. Gomes)

Abstract

In recent years, there has been significant interest from industrial and academic areas in the esterification of carboxylic acids catalyzed by acidic zeolites, as it represents a sustainable and economically viable approach to producing a wide range of high-value-added products. However, there is a lack of comprehensive reviews that address the intricate reaction mechanisms occurring at the catalyst interface at both the experimental and atomistic levels. Therefore, in this review, we provide an overview of the esterification reaction on acidic zeolites based on experimental and theoretical studies. The combination of infrared spectroscopy with atomistic calculations and experimental strategies using modulation excitation spectroscopy techniques combined with phase-sensitive detection is presented as an approach to detecting short-lived intermediates at the interface of zeolitic frameworks under realistic reaction conditions. To achieve this goal, this review has been divided into four sections: The first is a brief introduction highlighting the distinctive features of this review. The second addresses questions about the topology and activity of different zeolitic systems, since these properties are closely correlated in the esterification process. The third section deals with the mechanisms proposed in the literature. The fourth section presents advances in IR techniques and theoretical calculations that can be applied to gain new insights into reaction mechanisms. Finally, this review concludes with a subtle approach, highlighting the main aspects and perspectives of combining experimental and theoretical techniques to elucidate different reaction mechanisms in zeolitic systems.

Graphical Abstract

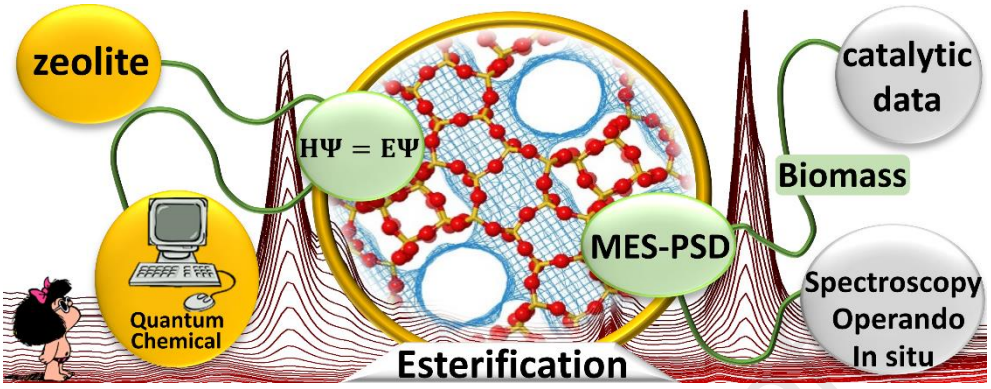

Keywords: Esterification; Solid acid catalyst; Confinement effects; In situ and Operando IR; Computational Catalysis; Theoretical Calculations

1. Introduction

The increasing demand for renewable energy across various sectors, including industry, transportation, and agriculture, coupled with government policies, has a significant positive impact on climate change mitigation. (Hashemizadeh et al., 2021; Khan et al., 2021a; Smirnova et al., 2021). In this context, biomass serves as a renewable resource for the production of biofuels and biomaterials, driving the development of innovative technologies. The conversion of biomass into products with high commercial value, in particular biofuels, involves feedstocks such as lipids containing triglycerides from animal fats, vegetable oils, microalgae, and oleaginous residues. Therefore, catalysis plays a crucial role in green chemistry processes by facilitating the conversion of platform molecules into diverse applications within the chemical industry, thereby reducing operational costs and minimizing environmental impacts.

Oleaginous biomass originates from various free fatty acids (FFA), organic compounds characterized by the presence of a carboxylic functional group (-COOH), along with an aliphatic chain of variable dimensions. Many oleaginous biomass conversion methods have been reported in the literature (Lilja et al., 2002; Gupta and Paul, 2014; Alaba et al., 2016; Dabros et al., 2018; Li et al., 2019; Tian et al., 2021; Satriadi et al., 2022); among which esterification stands out as a simple and low-cost process (Khan et al., 2021b) that is easily catalyzed by acid solids, such as modified mesoporous silica (Mutlu and Yilmaz, 2016; Cabrera-Munguia et al., 2017; Canhaci et al., 2023), sulfated zirconia (Rattanaphra et al., 2012; Patel et al., 2013; Raia et al., 2017), protonated zeolites (Chung and Park, 2009; Bedard et al., 2012; Vieira et al., 2013; Doyle et al., 2017; Vieira et al., 2017; Prinsen et al., 2018; Dal Pozzo et al., 2019; Gomes et al., 2019a), ion-changing resins (Martínez–Castelló et al., 2022; Sánchez-Correa et al., 2023), lamellar materials and inorganic oxides (Peters et al., 2006; Aranda et al., 2009; Lee et al., 2014). Esterification is also of paramount importance in organic synthesis, used in the solvent, drugs, lubricants, biofuels and derivatives of fine chemistry industries (Khan et al., 2021b; Ahmed and Huddersman, 2022). A Simplified diagram of the esterification process of carboxylic acids catalyzed by acidic zeolites to highlight the impact of the catalyst on the industrial process is shown in Fig. 1, illustrating the most important steps in the production of alkyl esters for different applications.

Among all the catalysts mentioned, acidic zeolites are highly advantageous, because of their robustness in different reactions (Ennaert et al., 2016; Zhang et al., 2022). Zeolites are crystalline aluminosilicates, consisting of well-ordered microporous with high activity and catalytic selectivity. These materials present

the possibility of modulating the electronic properties of the active sites, thus providing a wide variety of applications in catalysis and adsorption (Gong et al., 2022; Pérez-Botella et al., 2022).

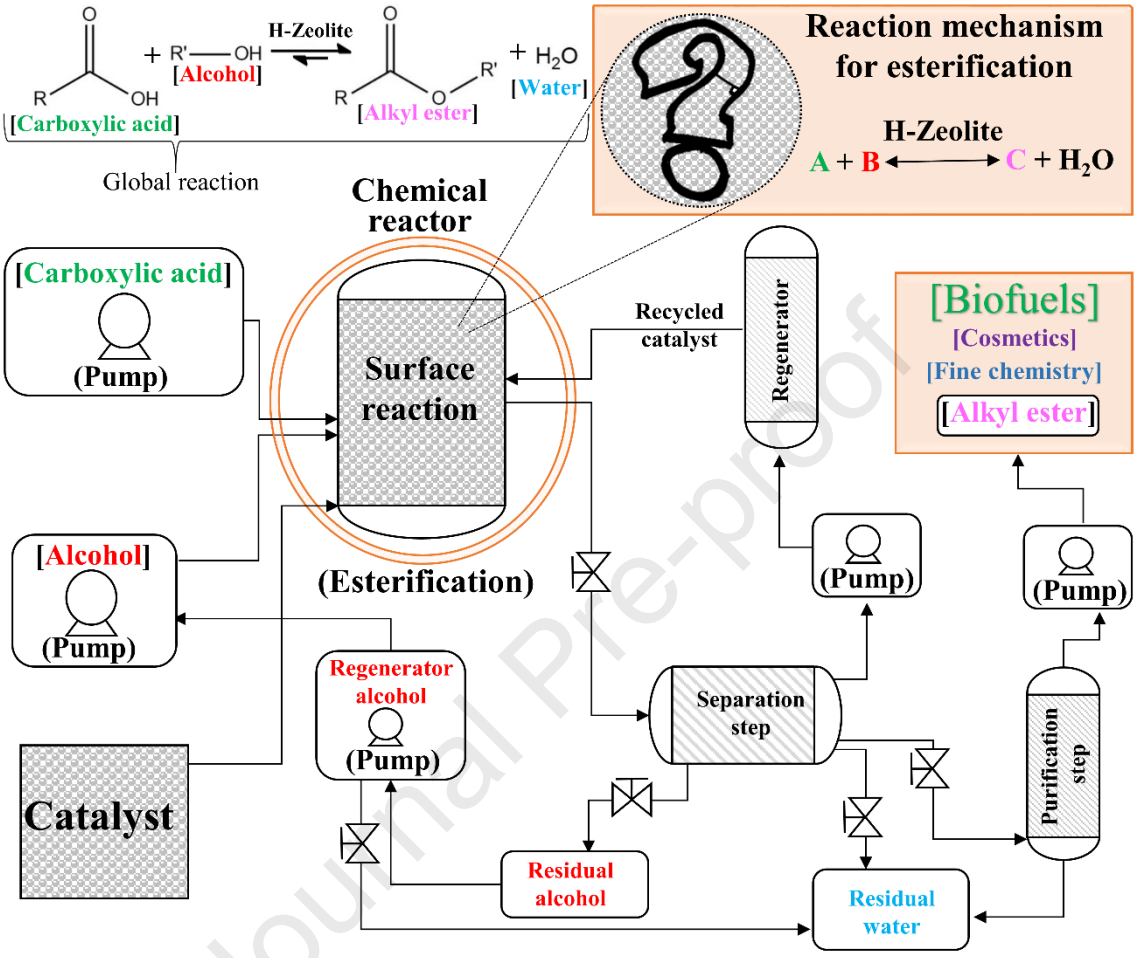

Fig. 1. Simplified flow diagram of an esterification process of carboxylic acids and alcohol catalyzed by acidic zeolites.

Many investigations on the esterification reaction catalyzed by acid zeolites (Kirumakki et al., 2004; Kirumakki et al., 2006; Chung et al., 2008; Aranda et al., 2009; Chung and Park, 2009; Lam et al., 2010; Chouhan and Sarma, 2011; Bedard et al., 2012; Fernandes et al., 2012; Atadashi et al., 2013; Vieira et al., 2013; Narkhede and Patel, 2014; Ciddor et al., 2015; Purova et al., 2015; Doyle et al., 2016; Ennaert et al., 2016; Doyle et al., 2017; Vieira et al., 2017; Prinsen et al., 2018; Dal Pozzo et al., 2019; Fattahi et al., 2019; Gomes et al., 2019a; Ketzer et al., 2020; Resende et al., 2020) make it possible to formulate new questions about the reactivity and selectivity in the formation of active intermediates during the reaction, since a catalytic behavior similar to that of a homogeneous catalysis could be expected.

Some studies suggest that zeolitic structures (pore diameter below 2 nm) are unsuitable for the esterification of carboxylic acids derived from large molecules with long alkyl chains (C_8–C_{18}) (Fernandes et al., 2012; Purova et al., 2015). The formation of intermediates and transition states (TS) is ultimately limited by steric effects caused by pores or cavities. On the other hand, other authors (Chung et al., 2008; Chung and Park, 2009; Vieira et al., 2013; Doyle et al., 2016; Vieira et al., 2017), suggest that the diffusion step is not the main limiting factor in the reaction, as evidenced by the good reaction yields for FFA under H-ZSM-5, H-MOR, and HY. Other factors influencing catalytic efficiency can be attributed to the steric effect, acid strength, hydrophobicity of the catalyst, and the relative adsorption of reactants and products on the active sites (Satyarthi et al., 2011; Bedard et al., 2012; Prinsen et al., 2018; Gomes et al., 2019a; Mowla et al., 2019; Fawaz et al., 2020).

Despite the large number of publications, controversy arises due to the complexity of the catalytic system, specifically the adsorbed species in confined void environments, as demonstrated by Gomes and co-workers for small model molecules adsorbed on H-Beta (Gomes et al., 2017) and H-ZSM-5 (Gomes et al., 2019b). Additionally, catalytic processes involving zeolites are highly complex, since many reactions in solid-gas, solid-liquid, or solid-liquid-gas phases occur in undefined places on the surface of solid catalysts. Consequently, it becomes difficult to determine the active sites, which are often generated only under real operando conditions (Corma, 2016). On the other hand, TS selectivity is governed by solvation inside confined voids, promoting the stability of active intermediates through numerous attractive dispersion forces. This effect has recently been observed in carbonylation on H-MOR, in which the proposed mechanism operates through three pore architectures that synergistically act in differently confined environments to promote the mobility of the active intermediate (Chen et al., 2022).

A comprehensive understanding of the interactions at the catalyst interface is essential for the development of a robust design that can be efficiently explored through a combination of experimental techniques and electronic structure calculations. Computational chemistry has proven to be a valuable tool in projects dedicated to the use and synthesis of zeolitic catalysts in various chemical industry processes(Chen et al., 2021; Ma and Liu, 2022). However, there remains a scarcity of atomistic-level knowledge regarding the specific use of such catalysts in biomass conversion. Further investigations are required to deepen our comprehension of the underlying mechanisms and to optimize the performance of zeolites in biomass-related reactions.

While, previous reviews discuss different topics such as heterogeneous catalysis for sustainable biodiesel production via esterification and transesterification (Endalew et al., 2011; Lee et al., 2014), zeolites in the catalytic conversion of biomass (Ennaert et al., 2016), heterogeneous mesoporous acid catalysts for esterification of free fatty acid raw materials (Soltani et al., 2017), zeolite-based catalysts for obtaining esters via esterification and transesterification (Fattahi et al., 2019), zeolite-catalyzed biomass conversion to levulinic acid and 5-hydroxymethylfurfural (Yan et al., 2023)and the synthesis of levulinate esters from carbohydrates (Shan et al., 2023). However, these works do not address crucial aspects such as the elementary steps and confinement effects of zeolites on the reaction mechanism, alternative techniques for identifying reaction intermediates, and computational calculations to help understand the reaction mechanism.

In this review, we investigate the different mechanisms proposed for esterification reactions in acidic zeolites. Furthermore, we show how the integration of infrared (IR) spectroscopy experiments and atomistic calculations can provide valuable information about the formation of active intermediates within confined environments. By combining experimental and computational approaches, we gain a deeper understanding of the intricacies of esterification reactions in acidic zeolites, shedding light on their catalytic behavior and potential applications in the field of organic synthesis. To achieve this goal, this review has been divided into four sections: The first is a brief introduction highlighting the distinctive features of this review. The second addresses questions about the topology and activity of different zeolitic systems, since these properties are closely correlated in the esterification process. The third section deals with the mechanisms proposed in the literature. The fourth section presents advances in IR techniques and theoretical calculations that can be applied to gain new insights into reaction mechanisms. Finally, this review concludes with a subtle approach, highlighting the main aspects and perspectives of combining experimental and theoretical techniques to elucidate different reaction mechanisms in zeolitic systems.

2. Zeolitic Catalysts

2.1. Topology vs active site

Zeolites are inorganic crystalline microporous materials that can be either found in nature or synthesized; they are usually composed of Si and Al with a tetrahedral arrangement linked by oxygen atoms, forming three-dimensional networks containing channels and cavities of different molecular dimensions (Corma, 1997; Li et al., 2015; Liang et al., 2021). Currently, the structure commission of the International

Zeolite Association (IZA) recognizes over 255 types of zeolites (Zhang et al., 2023). However, theoretical studies indicate a multitude of possibilities for synthesizing zeolitic frameworks, suggesting a promising pathway for the design of new materials (Schwalbe-Koda et al., 2021).

These structures exhibit high specific surface area, thermal stability, and the possibility of ionic exchange. As a result, the microporous inside different zeolitic systems function as microreactors, benefiting from improved selectivity and activity derived from the structural topology of these inorganic solids (Corma, 2016; Ennaert et al., 2016). This characteristic has generated significant interest in utilizing zeolites as acidic catalysts (Zhang et al., 2020; del Campo et al., 2021; Liang et al., 2021; Boronat et al., 2022).

Such protonated materials behave as solid superacids with acidity rates compared to those of H_2SO_4 (Umansky et al., 1991; Ben Mya et al., 2018). However, differently from other acid catalysts, such as metal oxides containing Brønsted acid sites (BAS), the strongest acid sites in zeolitic systems are generated in confined void environments (Fig. 2), through the replacement of Si atoms by trivalent metal atoms, such as Al^{3+} resulting in a negative charge on the structural lattice, that is counterbalance by a proton (Corma, 1995; Gorte and White, 1997; Corma, 2003).

The strength adjustment of acid sites can also be modulated by the isomorphic replacement of Al^{3+} by Ga^{3+}, Fe^{3+}, B^{3+}, Be^{2+}, Zn^{2+}, Ge^{4+}, Ti^{4+}, and Sn^{4+} (Li et al., 2015; Shamzhy et al., 2019; Opanasenko et al., 2020), once the composition of tri- and tetravalent heteroatoms has influence on the acid strength, allowing to adjust the acidity of the zeotype and thus adapt the catalyst properties as a function of the desired reaction (Jones et al., 2014; Creci et al., 2021). In addition to the acid strength, the topology of pores, channels, and cavities contributes to the stabilization of TS and the formation of intermediates inside these structures. The confinement of the pores can significantly influence the electronic structures of the species adsorbed by van der Waals (vdW) and electrostatic interactions, being able to compensate the intrinsic acidic strength of the zeolites (Xiao et al., 2021). Therefore, by combining the strength of acidic sites and the confinement effects, two effects can be observed: (i) electrostatic and covalent effects responsible for the strength of active sites in the catalytic process, and (ii) vdW interactions resulting from the confined void environment (Deshlahra and Iglesia, 2020).

The catalytic activity of BAS in confined environments (see Fig. 2) is generally described by the deprotonation strength, which is often used in the interpretation of reaction mechanisms; however, experimental techniques for measuring acidity in zeolites using probe molecules are challenged by several

233 factors, including confinement effects and interactions between probe molecules and Brønsted acid sites.
234 In addition, acidity heterogeneity within the same zeolite structure can also affect acidity measurement. It
235 is therefore important to consider these factors when performing acidity measurements on zeolites using
236 probe molecules (Boronat and Corma, 2015, 2019).
237

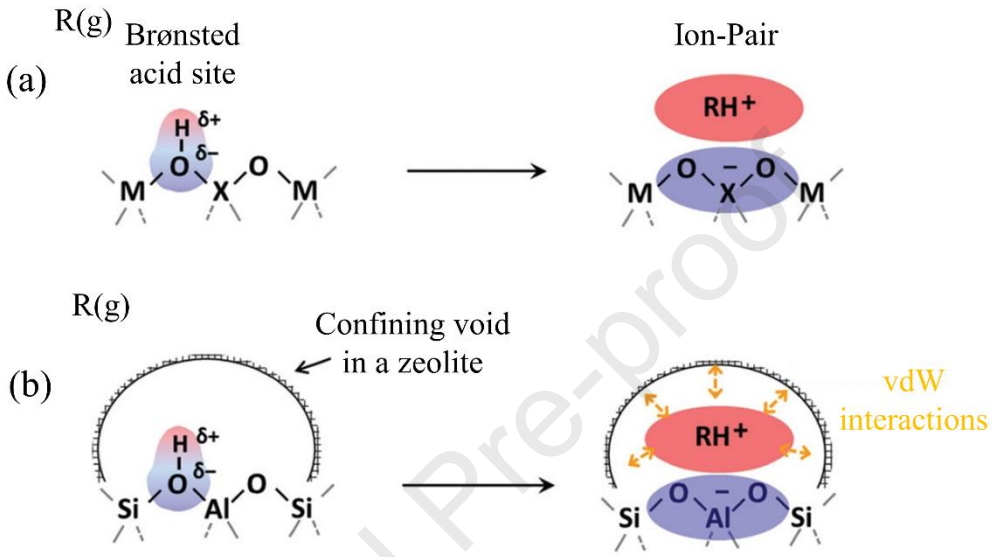

238

239 **Fig. 2.** Formation of cation–anion pairs in reactions of gaseous molecules (R(g)) at solid Brønsted acid sites
240 attendant to (a) unconfined heteroatom embedded in a metal oxide and (b) aluminosilicate with confining
241 void environments. Identities of the heteroatom (X) and the metal atom (M) in (a) influence acid strength
242 and ion-pair interactions while void structures influence van der Waals stabilization of molecular species,
243 from Deshlahra and Iglesia (2020).
244

245 Different types of O-H groups can be observed in the structure of aluminosilicates, implying a complex
246 catalytic system, as shown in Fig. 3. Some hydroxyl groups behave as BAS in zeolites, with different origins
247 and structures: bridging hydroxyl, nest hydroxyl, and terminal silanol groups (Zhai et al., 2017). The intense
248 Brønsted acidity can be located either inside pores and cavities, or on the external surface (Fig. 3. a, c).
249 Theoretical studies have shown that the deprotonation energy increases by 15-55 kcal mol^{-1} after the
250 relaxation of the geometry around the bridged O-H groups (Si-O-Al), which is an important parameter to
251 influence acidity (Boronat and Corma, 2015). It has recently been shown that the high acidity of the
252 hydroxyls in the zeolitic system may be related to the flexibility of the zeolite framework, which efficiently

accommodates the negative charge of the deprotonated center via structural relaxation, electron density redistribution, or hydrogen bond formation (Vayssilov et al., 2022).

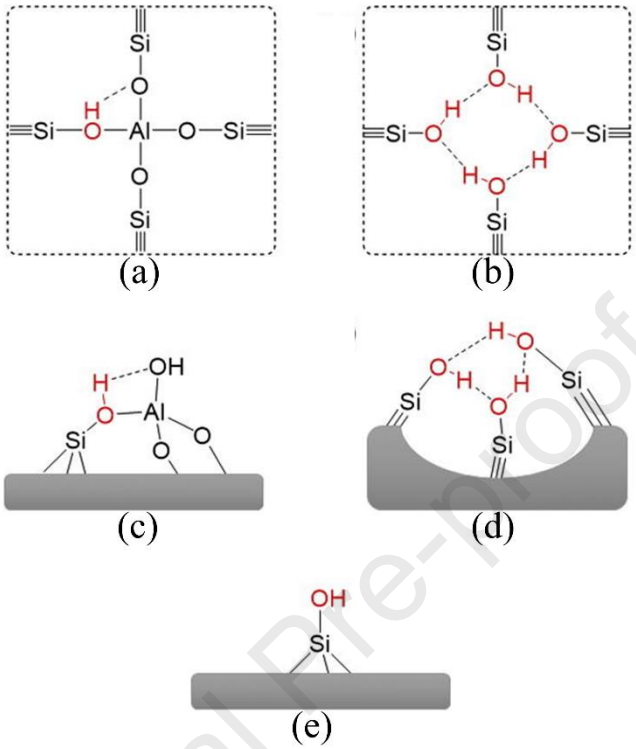

Fig. 3. Illustrations of (a) intra-crystalline bridging hydroxyl, (b) intra-crystalline hydroxyl nest, (c) bridging hydroxyl on an external surface, (d) hydroxyl nest on an external surface and (e) external surface terminal silanol, from Zhai et al. (2017).

Additionally, the use of mesoporosity to generate less mass transfer effects, greater thermal stability, and to adjust the acid strength of active sites has been widely explored in the literature through bottom-up methods and heat treatments (Verboekend and Pérez-Ramírez, 2011; Opanasenko, 2018; Jia et al., 2019); these strategies result in numerous structural defects forming hydroxyl nests inside the pores and cavities as well as on the external surface (Fig. 3. b, c) due to the removal of Si^{4+} or Al^{3+} ions. However, extra-lattice aluminum species (Fig. 3 c) are also generated on the surface of these inorganic solids, and these species favor higher catalytic activity in specific reactions (Arca and Mota, 2018; Han et al., 2020).

Understanding of acid catalysis heavily relies on the accurate identification of different types of acidic sites (as shown in Fig. 3) and their relationship to the structure of microporous aluminosilicates. In this context, the use of solid-state nuclear magnetic resonance spectroscopy (Yi et al., 2021; Peng and Tsang, 2022), the combination of gravimetric and IR analysis (Zholobenko et al., 2020), and the calculation of

deprotonation energy by computational modeling (Zhai et al., 2017; Trachta et al., 2022), provide highly accurate qualitative and quantitative data on the local environment of acid sites in zeolitic systems.

Several studies on the reactivity of acidic zeolites have demonstrated that the structural topology, location, and distribution of active sites within the pores and cavities of these materials play a crucial role in understanding catalytic activity and selectivity (Corma, 1995; Vermeiren and Gilson, 2009; Kubička and Kikhtyanin, 2015; Ennaert et al., 2016; Resasco et al., 2016; Li et al., 2017; Sultana and Fujitani, 2017; Fawaz et al., 2020). It was shown that, although the apparent activation energies and enthalpies for propene conversion over single and proximate protons were similar, the apparent entropy was lower for closer active sites, suggesting a lower energetic barrier due to steric constraints for the carbenium ion intermediates bound to nearby sites (Tabor et al., 2019; Hoffman et al., 2020). This effect can control the dissociative and associative reaction pathways, as demonstrated by Golabeck for the dehydration of alcohols (Gołąbek et al., 2020). In addition, aluminosilicates with a higher Si/Al ratio exhibit greater efficiency in liquid-phase reactions than other materials with a high Si/Al ratio due to hydrophobicity and greater thermal stability (Li et al., 2015; Jamil et al., 2020).

Despite the challenge of understanding zeolites acidity, theoretical information at the atomic level about the formation of the different acid sites suggests that the strength of a particular acid site can be increased by hydrogen bonds or long-range electrostatic interactions, associated with the geometry related to the location of the active site and the accessibility to O-H groups dependent on the orientation inside the pores (Zhai et al., 2017). However, the deprotonation energy related to BAS is the result of a refined interaction of structural, electrostatic, and electronic effects, observed only through quantum chemical calculations (Boronat and Corma, 2019; Rybicki and Sauer, 2019; Vayssilov et al., 2022). While the simulated deprotonation enthalpies for silanols range from 1186 to 1376 kJ mol^{-1}, those for BAS range from 1113 to 1187 kJ mol^{-1} (Vayssilov et al., 2022). The strong acidity of zeolite systems can be explained by the flexibility of the zeolite framework, which enables it to efficiently accommodate the negative charge of the deprotonated center through structural relaxation.

2.2. Diffusion in zeolites

As shown in Fig. 4 a, zeolites with pores diameters close to 4-7.5 Å formed by 8, 10, and 12 member rings (MR) are well explored in the transformation of hydrocarbons because their pores have diameters that are compatible with the size of refined hydrocarbons in the petrochemistry industry (Shi et al., 2015b). In

the specific case of sodalite zeolites (see Fig. 4 a. **SOD**), pores that are only 0.28 nm in diameter will inhibit the catalytic process, eliminating the possibility of bulky reagents diffusing through the pore and reacting with the active sites within the catalyst. Thus, the limitations on mass transfer involving zeolitic systems play an important role in the overall reaction rate.

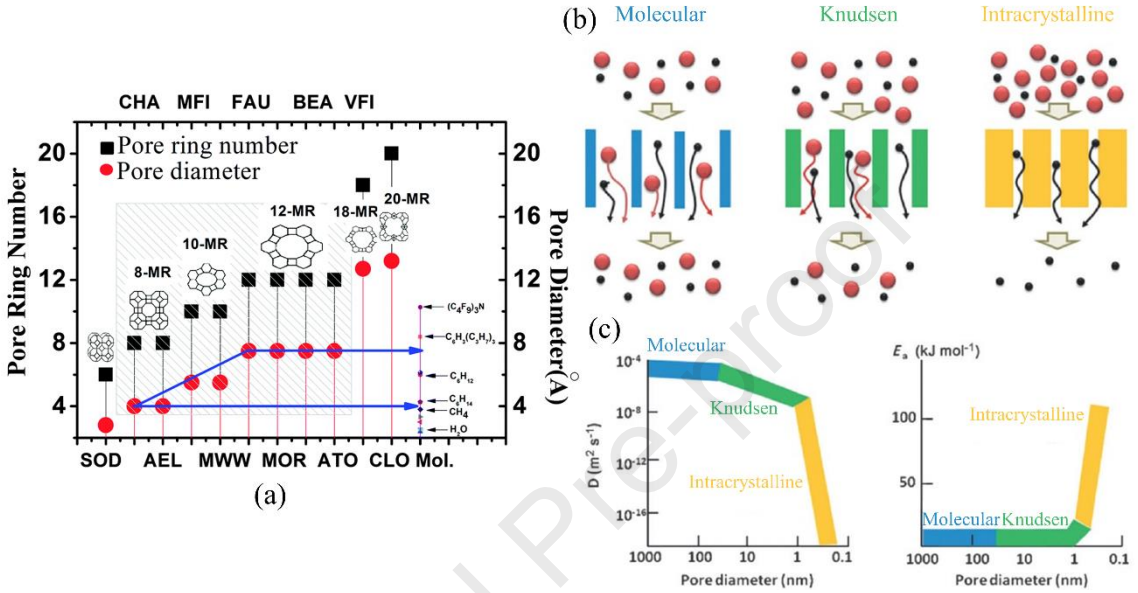

Fig. 4. a) Relationship of molecular diameter, pore diameter and pore ring number of different zeolites from Shi et al. (Shi et al., 2015b). Representation of the effect of pore size on the diffusion of large (red) and small (black) molecules. b) Effects of pore diameter on molecular diffusivity and of the energy of activation on diffusion from Li et al. (2014).

Bulky molecules are prevented from having free access to active sites inside the inorganic solid microporous due to the molecular sieve effect. In turn, molecules with access to the pores and cavities of the zeolites undergo diffusion processes by migrating towards the active centers within the pores (Fig. 4b); three classical types of diffusion can be observed: molecular, knudson, and intracrystalline diffusion.

The diffusion of perfectly fitted molecules into the microporous of zeolites is described as intracrystalline diffusion, or configurational diffusion, and is often observed to control molecular traffic within microporous solids (0.1-1 nm). It is highly dependent on reactants, type of zeolitic framework (tortuosity of the confined spaces), and temperature.

As the size of the molecules becomes similar to that of pores, the diffusivity decreases sharply to become smaller than molecular or knudsen diffusion (See Fig. 4 c) (Li et al., 2014). In the specific case of

intracrystalline diffusion, diffusivity is inversely proportional to the activation energy, which indicates that temperature is an essential factor in the diffusion process in zeolitic systems. At low temperatures, the reaction rate is unrestricted by diffusion resistances, and the observed activation energy represents the true value. At high temperatures, however, the reaction rate is hindered by diffusion resistances, resulting in an activation energy that is half of the true value (Hartmann et al., 2016).

In addition to the diffusion modes presented in this perspective, the ultrafast transport (hyperloop-like diffusion) of adsorbates in confined spaces has recently been observed for long-chain alkanes and one-dimensional zeolites (Yuan et al., 2023). In this situation, rapid diffusion was achieved when the long-chain molecules maintained their linear structure and operated in the center of the channel. However, this effect is not expected to be relevant in esterification reactions involving molecules derived from FFA's. Unlike alkanes, carboxylic acids have more reactive functional groups, and bulky FFA have unsaturation that results in collisions inside the pores. It is important to emphasize that the applicability of this model so far is limited to zeolites with monodirectional pores: the same transport process has not been observed in three-dimensional structures.

The diffusion process can be explored using a relationship between particle size and catalytic activity through the Thiele modulus (Φ) (Thiele, 1939). Low Φ values ($\Phi < 0.4$) are characteristic of reactions limited by kinetics, with the chemical reaction rate at the surface of the catalyst being lower than that of the diffusion. On the other hand, reactions with high Φ values indicate that the diffusion process is the limiting step. In this context, the morphological properties of different zeolitic systems have a far-reaching effect on their industrial applications, providing high shape selectivity for these microporous materials.

Many investigations have presented new strategies based on post-synthesis treatment (top-down strategies) or during zeolite synthesis (bottom-up strategies) to modify the structure of different zeolitic systems in order to optimize selectivity and decrease the diffusive effects in different reactions (Verboekend and Pérez-Ramírez, 2011; Hartmann et al., 2016; Bai et al., 2019; Shamzhy et al., 2019; Kerstens et al., 2020; Weissenberger et al., 2021; Silva et al., 2022; Yang et al., 2022; Zapelini et al., 2023). These studies show that zeolitic frameworks with additional porosity favor the reduction of mass transfer problems associated with conventional microporous systems, resulting in lower steric hindrance for bulky molecules; moreover, the pore blocking effect caused by coke species deposited on the surface can be minimized, providing higher efficiency and a longer lifetime in zeolitic catalysts. Recently, these effects were demonstrated for the production of methyl esters from the esterification of oleic acid and methanol on

desilicate H-MOR zeolite (Gomes et al., 2021). The authors reported that the hierarchical zeolite (H-MOR-D) showed higher conversion to oleic acid esterification than H-MOR (70% vs. 44%). Additionally, it demonstrated increased stability during reuse cycles, attributed to the higher accessibility of reagents to active sites located inside the pores.

2.3 Confinement effect on zeolitic frameworks

The confinement environment results in conformational distortions of both the inorganic solid structure and that of the adsorbed species inside the pores, affecting the reaction kinetics (Derouane, 1986; Derouane et al., 1988; Derouane, 1998). The structure of these microporous solids schematized in Fig. 5 provides a unique confinement effect by maximizing vdW and Coulomb interactions.

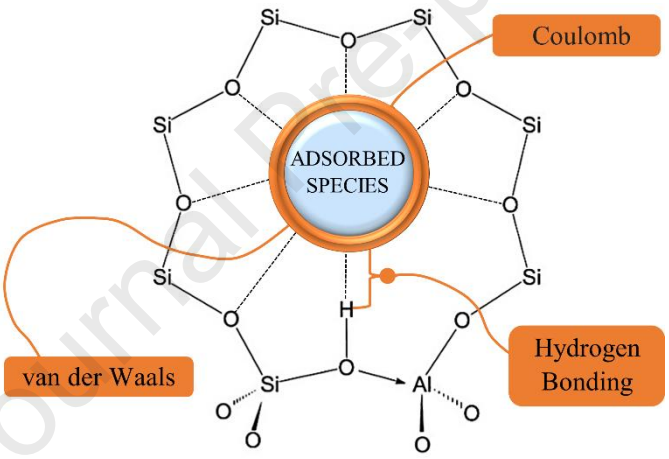

Fig. 5. Illustration to show the confinement environment in acidic zeolites. The species adsorbed inside the pores can interact with the zeolite surface via hydrogen bonding with the acid site, van der Waals interactions.

The spatial restriction inside the microporous increases the equilibrium constant of sorption and the concentration of chemical species (reagents, intermediates, and TS) on the active sites involved in the catalytic process (Derouane, 1986). This effect favors species that better interact with oxygen atoms, which constitute the zeolite framework, and may act separately or together with catalytic sites (Sastre and Corma, 2009; Sastre, 2016; Sultana and Fujitani, 2017). Therefore, when the zeolite pore diameter size is much larger than that of the adsorbed reagent size, the confinement effect becomes weak and may be significant

for bulkier adsorbates, forming a low electron density region between the cavity surfaces and the adsorbate (Fu et al., 2017).

The structure topology of pores and cavities in microporous systems makes zeolites act as solid solvents; as a result, the system is organized in a way that provides maximum stabilization to TS (Arca et al., 2014; Arca and Mota, 2018; Ozorio et al., 2021). Calculations based on the Density Functional Theory (DFT) showed that the confined environment around molecules adsorbed within the pores distorts to maximize vdW interactions through the interaction between the oxygens of the crystal lattice and the atoms of the adsorbed species (Sarazen and Iglesia, 2018). This effect is observed in the thermodynamic properties since the structural distortions of the inorganic solid recover enthalpy penalties while balancing the entropy losses associated with the rigid confinement. Other authors have compared the energy barriers between small and larger zeolite models calculated at the same level, where significant differences were found when confinement was considered (Sacchetto et al., 2015; Wen et al., 2016; Shen, 2017).

The confinement effect was demonstrated through DFT calculations by using two **MFI**-type zeolite cluster models of different sizes [small 8 T model (T = Si or Al), which represented the local properties of the active center, and a full pore structure 72 T model, which considers confinement], for the reaction of methanol to olefins (Zhang et al., 2016). The visualization of isosurfaces of reduced density gradient in real space can describe the noncovalent interactions between the reactants and the zeolite frameworks; thus, the effect of the vdW was observed in the stabilization of the TS, as shown in Fig. 6. Here it is suggested that the structure of the confined void environment favors more effective vdW interactions (green region in Fig. 6), which act in the stabilization of intermediates and TS, decreasing energy barriers. Clearly, the increased cluster size is beneficial for enhancing stability mainly through electrostatic interactions and vdW interactions (Tang et al., 2021).

Another work using DFT calculations and electron density analysis showed that for different types of zeolites (**MFI**, **BEA**), the large number of host-guest interactions found between the zeolite framework and the confined species are related to the energies involved in the reaction, differentiating the interactions related to the confinement effect from those related to the reaction on the active site (Zalazar et al., 2018b). Also, confinement effects play a crucial role in zeolites with large pore voids, such as Y zeolites where the stabilization energies of all species formed during the protonation reaction of styrene on H-FAU are significantly influenced by confinement effects, which are attributed to the weak host-guest interactions, besides the acid strength, as demonstrated by Zalazar et al., (2018a).

405

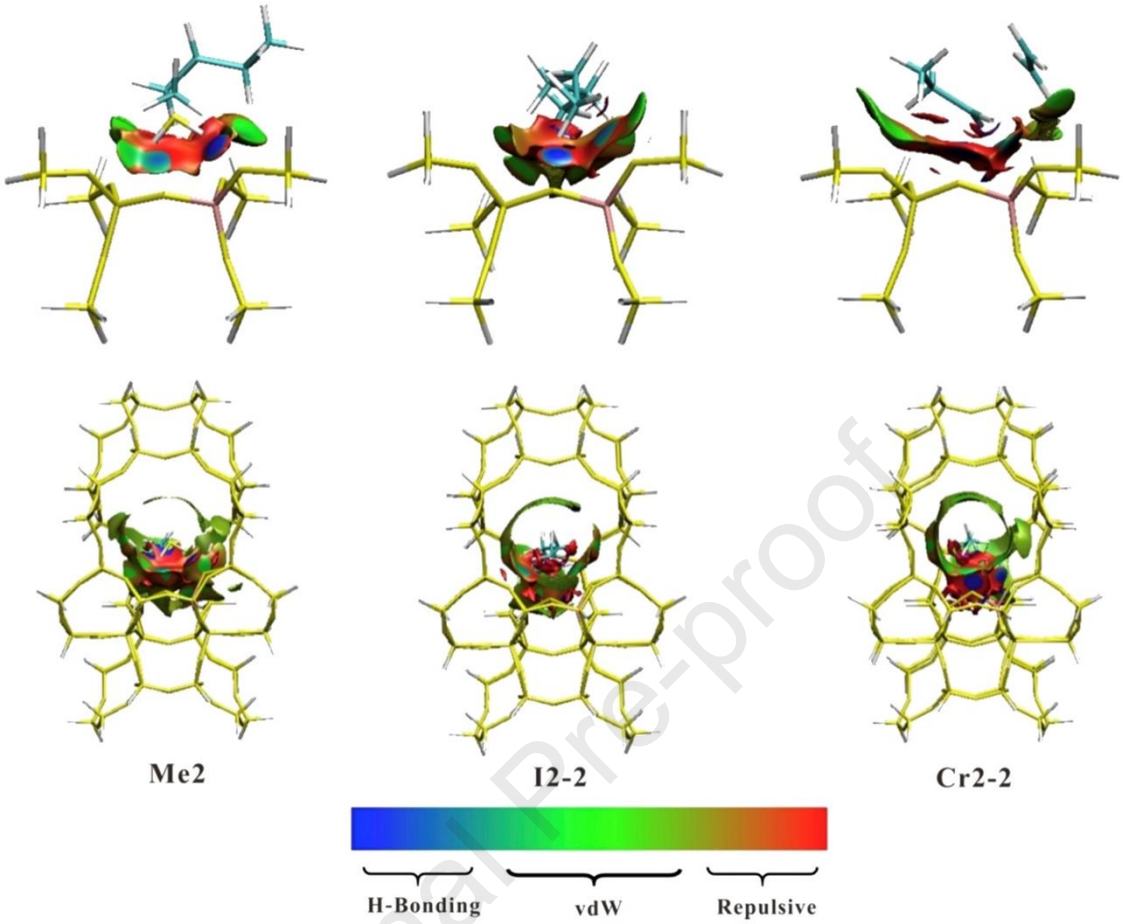

406

407 **Fig. 6.** Isosurface plots of reduced density gradient for the transition states species (confined in H-ZSM-5
408 zeolite) of C_5^+ formation from butene methylation (Me2), C_5^+ isomerization reaction (I2-2) and
409 C_5^+ cracking to ethene (Cr2-2). The isosurfaces of reduced density gradient are colored according to the
410 values of the quantity sign(λ2)ρ, and the RGB scale is indicated. vdW represents the van der Waals
411 interaction, from Zhang et al. (2016).

412

413 Different experimental and theoretical investigations show that the reactivity involving zeolites as
414 catalysts is the result of small changes in the size and shape of the confined spaces, which result in the
415 solvation of the TS and active intermediates; this behavior has been previously observed in classical
416 concepts of enzymes (Ferri et al., 2023). In the frame of this review, significant examples attesting the
417 importance of confinement effects in zeolite-involved reactions have been highlighted. This effect could be
418 of greater relevance in esterification reactions involving bulky molecules such as FFA, where the intricate
419 interplay between confinement, acid strength, and catalytic efficiency within the multifaceted realm could

maximize selectivity and catalytic activity. This concept can play a crucial role in specific chemical processes, ensuring greener catalysts for the conversion of industry-oriented platform.

3. Esterification mechanisms using micro-mesoporous acid catalysts

3.1. Mechanisms of esterification on the basis of kinetic studies

Catalysis involving zeolites follows the concept of heterogeneous reactions, which generally take place at the interface of a solid. The theoretical models of Pseudo-Homogeneous (P-H), Eley-Rideal (E-R), Langmuir-Hinshelwood (L-H), and Hattori are explored in the literature to understand heterogeneous catalysis (Weinberg, 1996; Heynderickx et al., 2020). These kinetic models, based on a fundamental reaction mechanism, are shown in Table 1 using mathematical equations to describe the process of esterification.

The P-H model (P-H, Eq. 1) assumes that reactions occur throughout the reactor volume, and that the concentration of the species on the catalyst remains constant, with no adsorption terms being considered for the species involved in the reaction. The E-R model (E-R, Eq. 2) suggests that the adsorption step controls the reaction rate (r_{ER}). In this case, the adsorption of the carboxylic acid on the active site generates a reactive intermediate to facilitate the reaction with the alcohol. On the other hand, in the L-H mechanism (L-H, Eq. 3), two reagents (carboxylic acid and alcohol) are adsorbed on the active sites, allowing the reaction to proceed with the adsorbed species. The Hattori mechanism (H, Eq. 4) combines elements of both the E-R and L-H models. In this mechanism, both reactants initially bind to adjacent active sites and then combine to form an intermediate surface complex bonded to only one active site.

These four kinetic models (P-H, E-R, L-H, and Hattori) were recently compared to describe the catalyzed oleic acid esterification reaction on USY zeolite and UiO-66 MOF (Chaemchuen et al., 2020; Ketzer and de Castilhos, 2021). Among the mentioned mechanisms, the E-R mechanism was accepted as an adequate model for the esterification of oleic acid with UiO-66 in this study based on the application of intrinsic initial reaction rate data. This model variant suggests that the surface reaction between the adsorbed oleic acid and methanol from the liquid phase is the rate-limiting step, and an additional active site is consumed to produce the ester and water as surface reaction products, so that a total of two active sites are used.

On the other hand, the analysis of the parameterization of the kinetic models for esterification, it was showed that the excessive number of parameters present in the E-R and L-H models (see Table 1 Eq. 2 and

450 3) can be related to a slight increase in the coefficient of determination (R^2) and a decrease in the objective
451 function values. The P-H model fit the experimental data better than the L-H or E-R models. However, it
452 is not possible to rationalize the discrimination of a reaction mechanism through this kinetic model because
453 it does not take into account the adsorption terms that influence the reaction kinetics (Tesser et al., 2010;
454 Zhou et al., 2020).
455

456 **Table 1.** Rate expressions based on elementary steps for the esterification reaction of oleic acid and
457 methanol over heterogeneous catalysts.

Kinetic models±	**Reaction rate expression**	**Eq.**
Pseudo - Homogeneous	$r_{PH} = k\left(C_{OA} - \frac{C_{MO}}{K}\right)$	Eq.1
Eley - Rideal	$r_{ER} = \frac{k\left(K_{OA}\,C_{OA}\,C_{MA} - \frac{K_{MO}C_{MO}C_{AA}}{k}\right)}{1 + K_{OA}\,C_{OA} + K_{MO}C_{MO}}$	Eq.2
Langmuir - Hinshelwood	$r_{LH} = \frac{k\left(K_{OA}\,K_{MA}\,C_{OA}\,C_{MA} - \frac{K_{MO}K_{AA}C_{MO}C_{AA}}{k}\right)}{(1 + K_{OA}\,C_{OA} + K_{MA}C_{MA} + K_{MO}\,C_{MO} + K_{AA}C_{AA})^2}$	Eq.3
Hattori	$r_H = \frac{kK_{OA}\,K_{MO}\,C_{tot}\left(C_{OA}\,C_M - \frac{C_{MO}C_w}{K_{eq}}\right)}{\left(1 + K_{OA}\,C_{OA} + K_M C_M + \frac{\frac{C_{MO*}}{C_{(MO)}C*}}{\frac{C_{MO*}C_W}{C_{(OA-M)}*}}.C_{MO}\,C_w + \frac{C_{MO*}}{C_{(MO)}C*}C_{AA} + K_W C_w\right)^2}$	Eq.4

Where C_{OA}, C_{MA}, C_M, C_{MO}, C_{AA}, and C_W are oleic acid, methyl acetate,methanol, methyl oleate, acetic acid, and water concentrations (mol dm^{-3}). The site balance is given by C_{tot}. The adsorption equilibrium constants of oleic acid, methyl oleate, methyl acetate, water, and acetic acid (L mol^{-1}) are denoted by K_{OA}, K_{MO}, K_{MA}, K_W, and K_{AA}. *K* is the equilibrium constant. *k* is the forward reaction rate constant (g_{cat}^{-1} min^{-1}). Surface intermediate (OA–M)*. ± (Chaemchuen et al., 2020; Ketzer and de Castilhos, 2021).

458

459 Corma et al., (1989) demonstrated that the mechanism of esterification of carboxylic acids with MeOH
460 catalyzed by H-Y involves, as a first preferential reaction step, the protonation of the carboxylic acid on
461 sites with strong acidity, followed by a nucleophilic attack by the alcohol. Similar results were observed
462 for the esterification kinetics of acetic acid (AA) and ethanol on MCM-41, demonstrating that AA needs to
463 be adsorbed on the surface and subsequently protonated for the formation of esters following the L-H-type
464 mechanism (Koster et al., 2001). However, these results were observed for mesoporous materials (MCM-
465 41), wherein the pore size permits the conformation of the double-site adsorption.

Investigations on liquid-phase esterification of AA with benzyl alcohol on different acidic zeolites (H-Beta, H-Y, and H-ZSM-5) have proposed a plausible reaction mechanism for esterification in zeolitic systems (Kirumakki et al., 2004). Scheme 1 represents the esterification mechanism adapted based on Kirumakki's investigation (Kirumakki et al., 2004).

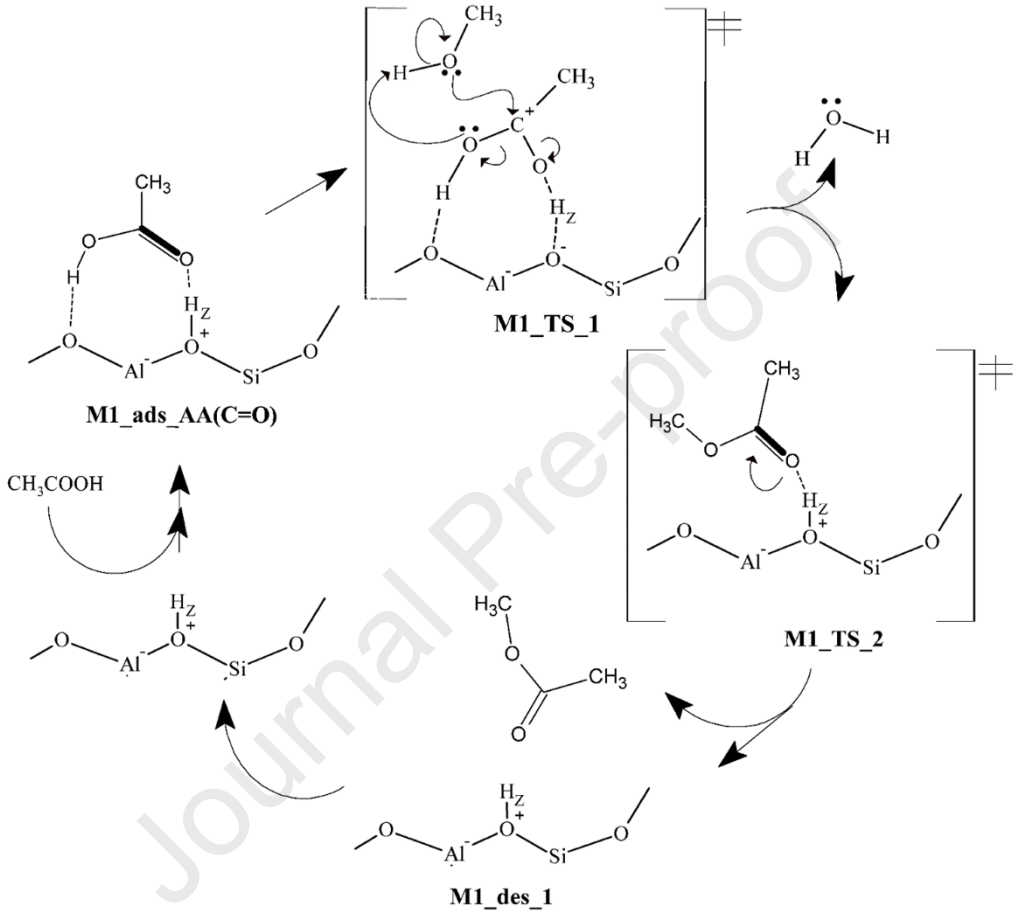

Scheme 1. Mechanism M_1 adapted for the esterification reaction of acetic acid and methanol on the Brønsted acid site in zeolitic systems from Kirumakki et al. (2004).

Esterification on BAS (Scheme 1, M_1) occurs through the protonation of the carboxylic acid (acetic acid molecule) as a chemisorbed acyl intermediate on the surface of the catalyst, which becomes electrophilic. In that mechanism, the adsorption of the carboxylic acid is stabilized by other oxygen atoms that constitute the crystal lattice of the aluminosilicate, thus acting as Lewis acids on the hydroxyl group of the organic molecule (M1_ads_AAC=O). Possible TS occurs through the nucleophilic attack of the alcohol, resulting in a water molecule and the stabilization of the acyl group on the proton (H_Z). In the subsequent

step, the ester formed on the BAS gives rise to the new TS (M1_TS_2), resulting in the desorption of the final product from the surface of the catalyst.

The mechanism proposed by Kirumakki is based on an E-R type mechanism, in which the reaction rate increases due to the concentration of a single species (acetic acid), regardless of the size of the alcohol molecule used in the experiment. This suggests a nucleophilic attack between the adsorbed carboxylic acid and the non-adsorbed alcohol as the rate-limiting step. In medium pore zeolites (ZSM-5 channels, 0.56 nm × 0.53 nm), the accessibility of bulky molecules to the active sites within the zeolite is unlikely, and this effect results in the inhibition of the formation of active intermediates and subsequent products. In this situation, the reaction is favored by zeolites with larger pores and cavities, such as H-Y and H-β (Jermy and Pandurangan, 2005; Kirumakki et al., 2006).

In later studies of the esterification kinetics between AA and methanol (MeOH) in SBA-15 functionalized with propylsulfonic acid, Miao and Shanks (2011) observed that the adsorption of MeOH leads to a significant decrease in the reaction rate, whereas the adsorption of AA or AA-MeOH leads to a significant increase in the reaction rate, suggesting the predominance of the L-H mechanism. This study clearly demonstrates the prevalence of AA adsorption, similar to what is observed in zeolite systems, where the E-R mechanism prevails. However, these intriguing observations raise pertinent questions about the specific intermediate steps that exert influence over the overall reaction.

Subsequently, Bedard et al. (2012) analyzed the esterification reaction of AA in the gas phase with ethanol on different types of acidic zeolites (H-BEA, H-FER, H-MFI, and H-MOR) and, through kinetic studies, proposed a new mechanism (M_2) that proceeds through a surface acetic acid/ethanol co-adsorbed complex involved in the rate-determining reaction step. In their study the author describe in detail the reaction pathways for the formation of stable intermediates in the adsorption step (Scheme 2). Briefly, (I) the first route initially involves the interaction of an alcohol molecule with the protonated surface of the catalyst, forms a stable intermediate (ethoxide) to react with an AA molecule in the gas phase, and giving rise to a coadsorption complex that will later result in the ester and water formation.

A second route (II) would be that, instead of the ethanol molecule being adsorbed on the surface of the protonated zeolite, first there would be the adsorption of AA on the surface of the catalyst. The adsorption of the acid molecule occurs via the hydroxyl group, forming one interaction with the BAS and another one with the adjacent oxygen belonging to the zeolite framework. The ethanol addition on the adsorption

complex (adsorbed acid) leads to an intermediate (III) that is dehydrated as the mechanism proceeds, resulting in the formation of ethyl acetate.

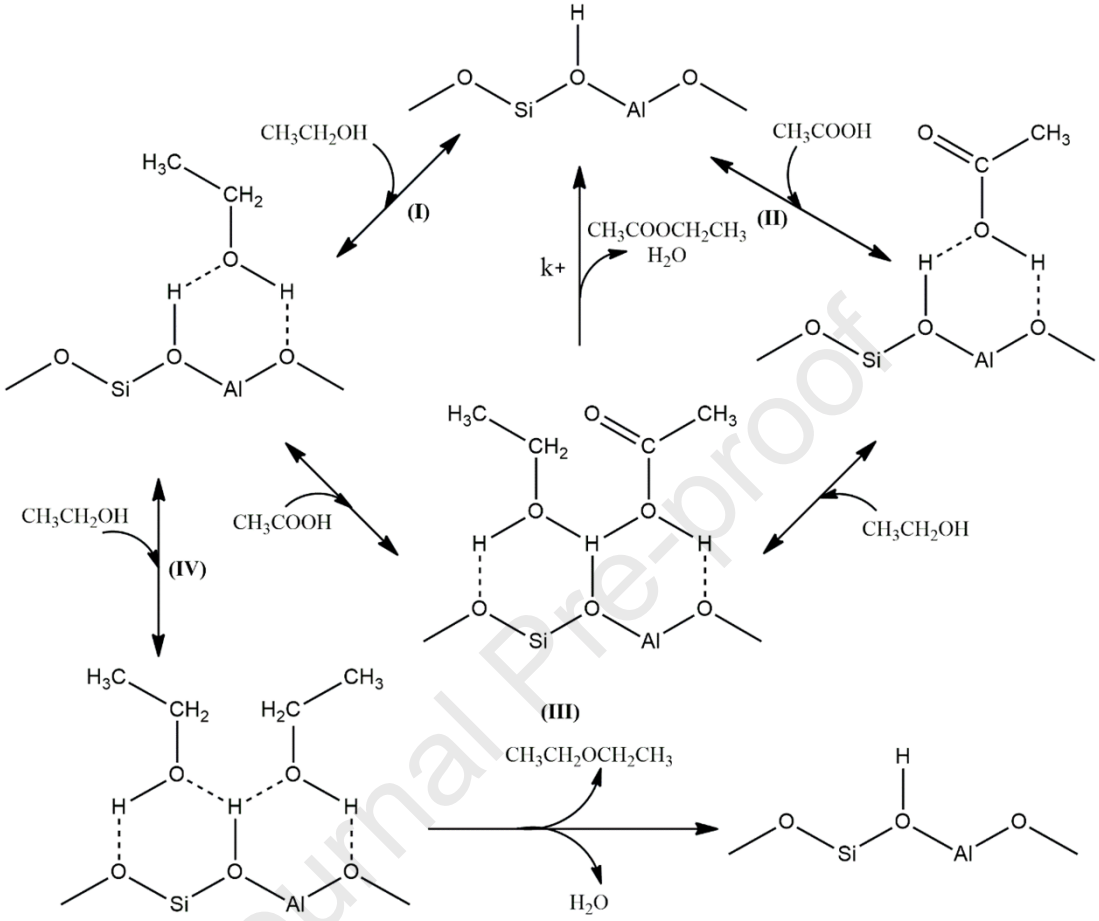

Scheme 2. Mechanism M_2 for the esterification reaction of acetic acid and ethanol on protonated zeolites from Bedard et al. (2012).

Both adsorption routes (I and II) lead to a stable intermediate (III), suggesting the H_Z sharing in a coadsorption process in which the two reactants (alcohol and acid) are both adsorbed on the surface of the catalyst, similarly to the L-H mechanism. This effect demonstrates that alcohol adsorption (route I) can be disregarded, since experimentally there is a negative dependence on the reaction rate of ethyl acetate in the presence of ethanol. However, under the same conditions for AA, the reaction rate of ethyl acetate becomes positive, indicating the existence of a co-adsorbed complex, in which both the alcohol and the acid must be present in the adsorption step of the esterification of carboxylic acids over BAS (Bedard et al., 2012). The authors also propose a route IV for the formation of ethanol dimers, which does not result in the formation of the desired product. In that study, the adsorption of reagents on the active sites of different zeolite

526 frameworks can be questioned, since it would be the limiting step of the esterification reaction on
527 microporous acidic solids.

528 Subsequently, Isernia (Isernia, 2014) proposed an adsorption mechanism for fatty acids on zeolitic
529 systems treated at high temperatures (800 - 1000 K). In this case, the sorption is induced through the London
530 dispersion forces of methyl groups (CH_3) of the carboxylic acid on the external zeolite surface. However,
531 this adsorption results in lower esterification reaction rates when compared to materials with high BAS
532 density. This catalytic process occurs in external sites with lower acid strength (Lakiss et al., 2020), which
533 implies low reactivity.

534 In this context, it is observed that different studies propose different mechanisms for the esterification
535 reaction in acidic microporous and mesoporous based on kinetic studies in gas and liquid phases. According
536 to a review by Ciddor et al. (Ciddor et al., 2015) the accepted mechanism is the one proposed by Bedard
537 et al. (Bedard et al., 2012) (see Scheme 2). However, a careful review of various mechanism proposals in
538 the literature revealed that the adsorption step of AA could occur through the interaction of either the
539 carbonyl or hydroxyl group of AA with the BAS. Each possibility leads to different elementary steps in the
540 overall process. Consequently, obtaining a comprehensive understanding of the adsorption mechanism of
541 carboxylic acids and alcohols within the zeolite structure from catalytic data becomes an arduous task
542 because the kinetics of reactions involving numerous intermediates and elementary steps do not provide a
543 complete understanding. In addition, kinetic models are not sensitive enough to detect short-lived
544 intermediates. Thus, the ability to discern the effects of zeolite structure on esterification kinetics depends
545 on the decomposition of elementary steps along with the simultaneous description of the effects of spatial
546 constraints on the stability of adsorbed intermediates.

547

548 3.2. Complementary studies of the mechanism of esterification based on theoretical calculations

549

550 From an atomistic point of view, the study of the adsorption mechanism becomes much more complex,
551 as it involves the energetic analysis of different molecular conformations (adsorption modes) that come
552 into play during the adsorption of reagents. In order to fully understand the different elementary steps of
553 adsorption (since in general all the discussions proposed that the adsorption step be the rate-determining
554 reaction step) according to the different mechanisms postulated in the literature (Kirumakki et al., 2006;
555 Bedard et al., 2012), a detailed study of these factors was carried out by Gomes et al (Gomes et al., 2017).

Their work resulted in an improved proposal for the adsorption mechanism by using IR spectroscopy, thermogravimetric analysis (TG), and theoretical calculations based on DFT (Scheme 3) (Gomes et al., 2017). The adsorption step for the esterification reaction on acid zeolites can either occur in two different steps or in a single step, giving rise to the AA/MeOH co-adsorbed complex involved in the rate-determining reaction.

The proposed mechanism implies that the adsorption complex of AA/MeOH on BAS can be formed in two ways, giving rise to two pathways for the formation of different adsorption complexes: (I) by the stepwise adsorption of an AA or MeOH molecule on the active site, followed by the coadsorption of a second molecule, resulting in an adsorbed complex formed in two elementary steps; or (II) by the concerted simultaneous adsorption of AA and MeOH on the catalytic site. In turn, AA could be adsorbed by a carbonyl or hydroxyl group, and depending on the adsorption mode, the mechanism may be different.

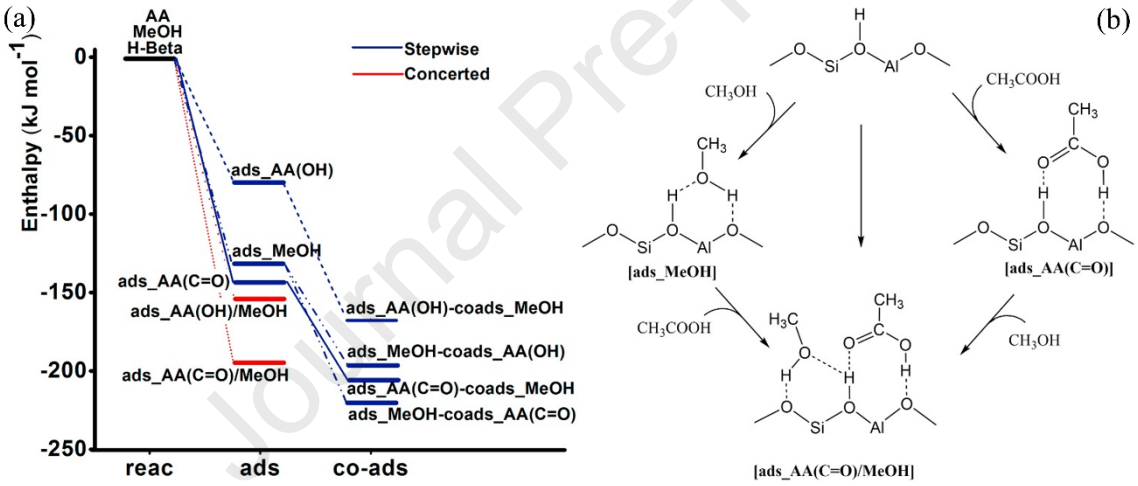

Scheme 3. (a) Enthalpy profile for the adsorption and co-adsorption of methanol and acetic acid on H-Beta zeolite calculated at M06–2X/6-31G(d) level. (b) Revised mechanism for the formation of the acetic acid/methanol adsorption complex from Gomes et al. (2017).

Considering the energetically more stable structures in the three ways to form the adsorption complexes (see Scheme 3 a), no significant differences were observed when comparing the energy magnitudes between the complexes that involve the AA adsorption [ads_AA(C=O), $\Delta H°$=-143.7 kJ mol^{-1}] and the MeOH coadsorption [ads_AA(C=O)-coads_MeOH, $\Delta H°$=-194.6 kJ mol^{-1}], and proton sharing as a one-step adsorption [ads_AA(C=O)/MeOH, $\Delta H°$=-194.6 kJ mol^{-1}] for BEA structures (Gomes et al., 2017); similar results were also observed for **MFI** structures (Gomes et al., 2019b). These results suggest that the

determining reaction step must involve these adsorbed complexes, in which AA interacts with the zeolite surface through the C=O group (as opposed to the mechanism proposed by Bedard et. al(Bedard et al., 2012), in which AA adsorption is through the hydroxyl group).

Analyzing the route II proposed by Bedard et. al(Bedard et al., 2012) (see Scheme 2), a new mechanistic scheme (see Scheme 4) becomes plausible, in which the adsorption of an alcohol (MeOH) could be the initial step.

The initial interaction occurs through the adsorption of MeOH on the BAS, forming two hydrogen bonds. One between the $H_Z \cdots O$ of alcohol and the other referring to the hydroxyl group with the zeolite crystal lattice, forming the M3_ads_MeOH complex, a widely explored step for other reactions (Van der Mynsbrugge et al., 2012; Van Speybroeck et al., 2014; Van Speybroeck et al., 2015; Piccini et al., 2018; Costa et al., 2019). The adsorbed complex can follow two distinct paths, which give rise to the formation of MeOH dimers (M3_ads_dimMeOH) or to a possible TS (M3_TS_1). In the case of the M3_ads_dimMeOH complex, H_Z can be solvated by alcohol molecules that interact with BAS, inhibiting the catalytic process in subsequent steps. It was reported that the adsorption of alcohol dimers onto H-ZSM-5 removes H_Z from the structural framework of the catalyst, resulting in the fluctuation of H_Z between the two alcohol molecules in dynamic equilibrium, thereby inhibiting the esterification process (Gomes et al., 2019b).

In M3_TS_1, alcohol protonation occurs for the subsequent formation of a water molecule and a methoxide intermediate, which undergoes a nucleophilic attack by the oxygen adjacent to the BAS, which in turn acts as a Lewis acid site, forming a methyl intermediate; in a second TS (M3_TS_2), such an intermediate could react with a carboxylic acid molecule adsorbed on the surface of the zeolite through the hydroxyl group, resulting in the sequence of mechanisms in the formation of an ester adsorbed on the zeolite and the regeneration of the acid site (see M3_des_1) for a new catalytic cycle.

The carbonyl protonation energy for carboxylic acids is a spontaneous process in a homogeneous acid medium, showing a lower energy barrier than that of protonation by the hydroxyl group, although the protonation rate also depends on spatial factors. The protonation of the carboxylic acid through the hydroxyl group favors the formation of the acyl ion, which is a highly active agent in the esterification reaction in a homogeneous medium (Shi et al., 2015a). However, the presence of the acyl ion in the confined environments of a zeolitic framework could imply a greater energy barrier in the initial steps of the mechanism and is not expected to be formed because the formation of the acyl cation lacks the assistance

of the framework's oxygen atoms for its stabilization, given that it would be positioned far from the surface of the zeolite (Fernandes et al., 2012). In this situation, the adsorption in steps or in a concerted mechanism is energetically favored by the carbonyl group, that is, the opposite of what occurs in a homogeneous medium.

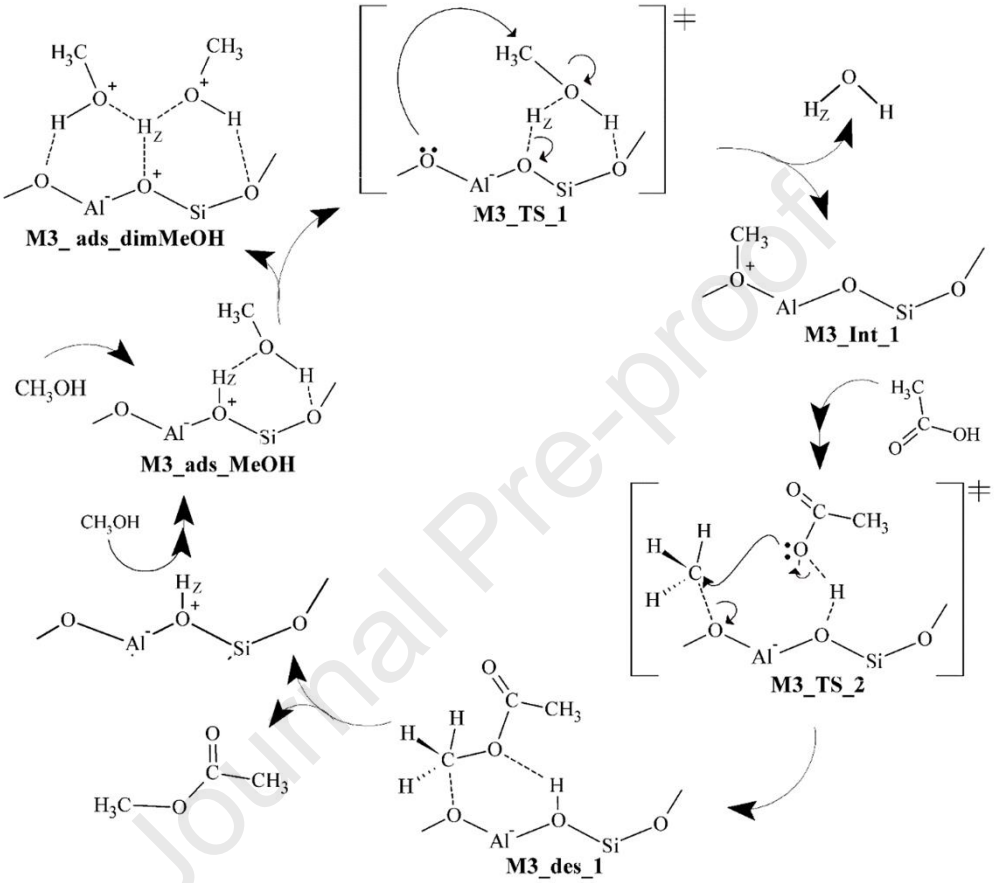

Scheme 4. Mechanism M_3 for esterification of acetic acid and methanol on Brønsted acid sites via methanol adsorption.

As mentioned at the beginning of this section, despite the enormous efforts made for the compression of the esterification mechanisms of carboxylic acids on micro-mesoporous solids, further discussion is required on the effect of different topologies of zeolites and the real role of active sites in FFA conversion.

3.3. FFA´s model molecules used in esterification catalyzed by acidic zeolites

The conversion of fatty acids into esters for various applications through zeolite-catalyzed esterification must be understood in order to optimize the process and achieve high conversions. In this sense, the use of model molecules in esterification makes it easier to carry out experimental and theoretical studies, since

626 they are smaller and more volatile, do not have the chemical complexity of residual oils and fats, and contain
627 the main functional groups. In addition, molecules such as acetic acid, levulinic acid, palmitic acid, and
628 oleic acid allow exploring their combinations with other molecules to form bulky intermediates, which can
629 present different types of interactions and conformations within confined environments.

630 In order to understand the catalytic performance of acidic zeolites in the conversion of palmitic acid,
631 Prinsen et al. (2018) compared the catalytic activity of the zeolites H-ZSM-5 and H-Y with different Si/Al
632 ratios in an esterification reaction in liquid phase under mild conditions of operation. The authors suggest
633 that the esterification must be mainly catalyzed by the BAS, through a proton transfer from the acidic sites
634 to the carbonyl oxygen of the AA and, consequently, the formation of a carbenium ion, followed by
635 nucleophilic attack of an alcohol molecule and subsequent deprotonation, dehydration, and formation of
636 the desired product. Similar results were observed in an in situ experiment on H-ZSM-5, which showed
637 that the formation of the ester of interest occurs via the electrophilic reaction of protonated acid (adsorbed
638 on zeolite) with alcohol (Mowla et al., 2018).

639 Also (Prinsen et al. (2018), demonstrated that pore size and hydrophobicity hold greater significance
640 than the density of strong acid sites (BAS) for facilitating the reaction process. This phenomenon can be
641 attributed to the fact that H-Y zeolites possess large supercage voids (1.3 nm) connected by 12-MR
642 windows (0.74 nm), while H-ZSM-5 zeolites have medium-sized microporous (ranging from 0.56 x 0.53
643 nm). Moreover, the density and accessibility of BAS were higher in H-Y compared to H-ZSM-5, which is
644 attributed to the majority of these active sites being located within the large supercage voids. The water
645 produced during esterification remains adsorbed on the surface of zeolites with a low Si/Al ratio. In a recent
646 study, using IR spectroscopy with **FAU**-type zeolites in sodium and acid forms it was found that the effect
647 of hydrophobicity is extremely important in liquid phase reactions, to avoid the deactivation of the catalytic
648 centers and favor the rapid desorption of surface water molecules, improving catalytic efficiency (Gomes
649 et al., 2019a).

650 In the case of H-ZSM-5, the average pore size (0.56 - 0.53 nm) does not promote the esterification
651 reaction of long-chain fatty acids (palmitic acid) inside the pores, as reported by Prinsen et al. (Prinsen et
652 al., 2018), the reaction occurs on the outer surface resulting in low conversions (less than 27% in esters).
653 Contrary to what has been found by some authors for H-ZSM-5 and H-MOR under similar experimental
654 conditions (reaction temperature = 60-100 °C, amount of catalyst = 1.0 g, reaction time = 1-3 h), with yields
655 above 60% for the esterification of oleic acid (Chung et al., 2008; Chung and Park, 2009; Mowla et al.,

2019; Gomes et al., 2021; Gomes et al., 2022). Such discrepancies shows that, experimentally, many questions related to the topology of different zeolitic systems need to be explored at the atomistic level to fill the gaps and provide accurate information on the application of these materials in esterification. In summary, based on the previously cited investigations involving protonated zeolites, only selected zeolite frameworks (**BEA, MFI, FAU**) present themselves as feasible candidates for catalytic implementation, which can be attributed primarily to diffusion constraints, hydrophobic influences, distribution and location of active sites. Consequently, the quantification of acidic sites and the determination of the catalyst's external surface area take on fundamental importance when assessing the catalytic efficiency within the context of the esterification process (Ribeiro et al., 2021).

Mowla et al. (2019) observed that the activation energy in esterification (24.8 kJ/mol for oleic acid and 46.7 kJ/mol for acetic acid esterification on H-β) is influenced by the reactant molecules size on the zeolitic system (**BEA** and **MOR**), resulting in reactions at the pore mouth in a case of large molecules. These results suggest that the hydrophilic nature of the catalyst causes a diffusional barrier for large molecules. The diffusive processes in zeolitic systems can be minimized by the effect of temperature and the miscibility of the acid-alcohol faces, which favor higher reaction rates due to the disappearance of mass transfer resistance (Vieira et al., 2013; Fereidooni et al., 2021). However, for some zeolitic frameworks, the step of controlling the esterification reaction rate occurs through kinetic processes (Mowla et al., 2019; Ketzer and de Castilhos, 2021).

On the other hand, unlike conventional zeolites that are predominantly microporous, hierarchical zeolites contain an additional mesoporous structure, which reduces diffusion limitations (Chen et al., 2020). The mesopores enhance the reagent diffusion and influence the reaction mechanism by allowing better accessibility for bulky molecules inside the pore, thus reducing steric hindrance. Consequently, these structures exhibit excellent catalytic performance in the liquid phase reaction due to their low resistance to diffusion.

Mitran et al. (2021) demonstrated that different acid sites within β zeolites fulfill distinct functions in esterification, specifically with propionic acid. While the external silanol groups (Si-OH) exhibit weak acidity, the Si-OH-Al groups exhibit strong Brønsted acidity, and the silanol nests associated with the defect sites exhibit Lewis acidity. It was observed that the zeolite exhibiting the highest specific surface area, the highest volume of mesoporous, and the highest Brønsted acidity positively influenced the lowest energy barrier. Similarly, Fawaz et al. (2019, 2020) analyzed different crystal morphologies of H-ZSM-5 zeolite

crystals in the linoleic acid esterification process and discovered a correlation between diffusive properties and catalytic performance. As a result, approximately 80% conversion rates can be attributed to reactions taking place at the pore entrance and outer surface. These findings suggest a synergy between hierarchical porosity and acidity.

A recent study (Fawaz et al., 2021) investigated the use of different hierarchical structures of H-ZSM-5 zeolite for the conversion of waste frying oils, resulting in conversions below ~50%. This highlights the importance of precise localization of active sites and the impact of mesoporosity on diffusion effects. Consideration of contaminants in waste oils, which can affect crucial steps such as competitive adsorption among reagents, is particularly important.

More recently, a combination of experimental studies and theoretical calculations has revealed that mobility restriction in **MOR**-type zeolitic frameworks can significantly affect the esterification reaction of bulky carboxylic acids (Gomes et al., 2021). It has been shown, at the molecular level in Fig. 7, that this effect does not occur in **FAU**-type structures. For AA, the space within the 12-MR pore allows the free mobility of small molecules (MeOH and AA). However, for bulky carboxylic acids, adsorption implies an additional rearrangement to favor the accommodation of the aliphatic chain extension and, consequently, provide a better spatial arrangement; such enhancement optimizes interactions with the crystalline structure of the catalyst causing distortions in the molecule, which provides a better fit over the active site. On the other hand, the extended length of the aliphatic chain of bulky FFA is repelled within the confined space, which limits rotational and translational movements within the catalyst pore, generating thermodynamic penalties. Thus, it is observed that the high conversions in zeolitic systems are related to molecular transport.

Table 2 shows the catalytic performance of different zeolite structures used for esterification of long-chain FFA's. It can be seen that most zeolites show high catalytic activity for different types of FFA's. **FAU**-type structures show conversions above 90%, although they have a lower density of active sites and are more accessible inside the pores and cavities than **MFI**, **BEA**, and **MOR**-type structures. In the case of the H-USY zeolite, the presence of strong BAS drastically affects the higher selectivity for oleic acid esterification with methyl acetate, requiring changes to acid sites of moderate strength to maximize conversion. On the other hand, the performance of **MFI** and **MOR**-type structures depends on the high density of acid sites. In these materials, the catalytic process can take place at the mouth of the pores, but

in **MOR**-type zeolites, the strong adsorption of reagents, intermediates, and products favors pore blockage, reducing the useful life of the catalyst and resulting in a slow reaction rate for many reaction cycles.

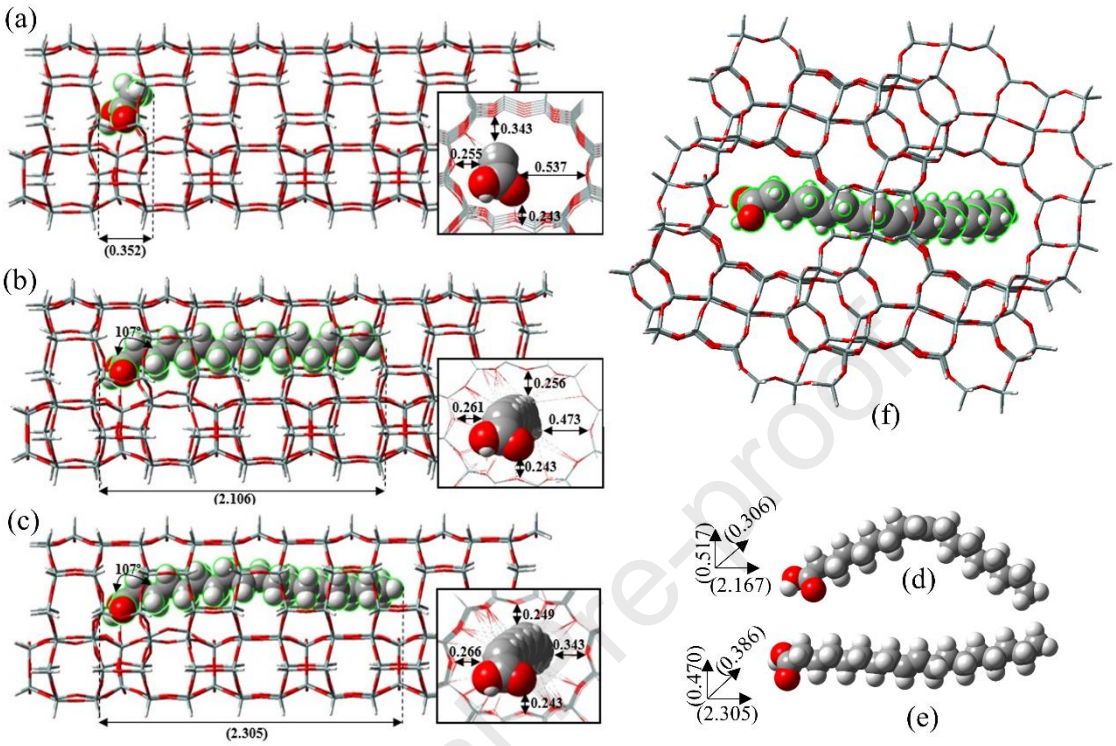

Fig. 7. Side view of the minimal energy complexes for different carboxylic acids in H-MOR calculated at ONIOM M06-2X/6-31G(d):PM6 level. a) adsorbed acetic acid; b) adsorbed palmitic acid; c) adsorbed oleic acid. Distances in nm. Minimum energy structure of oleic acid. d) Conformation for isolated oleic acid. e) Conformation of oleic acid in the 12-MR pore of the H-MOR zeolite. Structures calculated at M06-2X/6-31G(d) level, from Gomes et al. (Gomes et al., 2021). f) Adsorbed oleic acid on H-FAU zeolite cluster from et al. (Gomes et al., 2019a).

By observing the solvation effect reported in other studies (Gounder and Iglesia, 2013; Arca and Mota, 2018; Sarazen and Iglesia, 2018; Zalazar et al., 2018b; Mowla et al., 2019) the energy barrier should be lower for larger molecules, since they allow greater interactions with the surface of the inorganic solid. Thus, several factors are hence fundamental for the catalytic process involving zeolites, such as the steric effect, strength of acid sites, specific area, availability, and stability of active sites in confined voids, reagent polarity, hydrophobicity, and the structural shape of the catalyst, which can direct the breakdown of molecules of interest towards undesirable side reactions.

Table 2. Comparison of conversion of carboxylic acids over acid zeolite

Catalyst (Framework)	Alcohol : Feedstock	Temperature (°C)	Feedstock	Reaction time (h)	Conversion (%)	Ref.
H-ZSM-5 (**MFI**)	2:1	60	Soybean oil	1	~80	(Chung and Park, 2009)
	2:1	70	Palmitic acid	3	20-27	(Prinsen et al., 2018)
	6:1	180	Linoleic acid	4	86.4	(Fawaz et al., 2019)
	45:1	100	Oleic acid	4	55	(Resende et al., 2020)
	12:1	180	Waste frying oils	4	~50	(Fawaz et al., 2021)
	3:1	100	Oleic acid	5	70	(Gomes et al., 2022)
H-Y (**FAU**)	2:1	70	Palmitic acid	3	100	(Prinsen et al., 2018)
	6:1	68	Oleic acid	6	95	(Dal Pozzo et al., 2019)
	3:1	100	Oleic acid	4	98	(Gomes et al., 2022)
H-USY (**FAU**)	10:1	240	Oleic acid	1	66	(Ketzer et al., 2020)
H-Beta (**BEA**)	3:1	66	Oleic acid		75	(Mowla et al., 2019)
	3:1	100	Oleic acid	5	85	(Gomes et al., 2022)
H-MOR (**MOR**)	2:1	60	Soybean oil	1	~80	(Chung and Park, 2009)
	-	130	Palm oil	50	91	(Isernia, 2014)
	3:1	100	Oleic acid	2	~44	(Gomes et al., 2021)

The design and development of efficient catalysts depend on a deep theoretical and experimental view of the reaction mechanism and the relationship between catalytic activity and pore and cavity structures (Parangi and Mishra, 2020). With advances in computing, sophisticated theoretical calculations can help to elucidate unanswered questions about the mechanism of esterification catalyzed by acidic zeolites. In this sense, this experimental information can support robust analyzes on the nature of active sites during catalysis through spectroscopic characterizations operando and in situ.

4. IR spectroscopy and electronic structure calculations

Studies involving reaction mechanisms and the synthesis of new catalytic materials require precise methods for analyzing bulk and surface properties (Yi et al., 2021; Chen et al., 2022; Peng and Tsang, 2022; van Vreeswijk and Weckhuysen, 2022). In this sense, infrared radiation methods (ATR, transmission FTIR,

VTIR, DRIFT, among others) are essential tools for gathering information related to the interactions between organic and inorganic materials. These techniques allow the observation of phenomena occurring at frequencies in the order of 10^{13} and 10^{15} Hertz (Paul et al., 2018). Since the 1950s, IR spectroscopy has been a valuable tool in the study of numerous aluminosilicates, leading to significant advances in the understanding of both Brønsted and Lewis acid sites (Bordiga et al., 2015). In situ operando mode IR spectroscopy has been applied to various catalytic systems (Bordiga et al., 2015; Atzori et al., 2020; Bertella et al., 2020; Khalili et al., 2021; Nepel et al., 2021; Yuan et al., 2021), to identify active sites and intermediate species formed under real catalytic conditions. However, conducting IR spectroscopy experiments at the interface of a given catalyst proves to be challenging due to the difference in sensitivity of the species absorbing infrared radiation and the complexity of parallel reactions that lead to the formation of intermediates, spectator species, and products. Therefore, computational studies are required to distinguish the species of interest.

It is widely accepted that the active sites are not fixed in the crystalline structure of the different zeolite systems. Instead, they operate dynamically and can be mobilized within the pores or cavities of the respective zeolites under operando conditions (Bocus et al., 2021). In this sense, Tabor et al. (2019) used in situ IR and MAS NMR spectroscopy to study the effect of proton site distances on propene oligomerization and aromatization on H-ZSM-5. The results revealed the progressive formation of saturated alkaline and aromatic carbocations generated by the protonation of olefins and intermolecular hydride ion transfers. However, the polarization of the reactants and steric restrictions for the carbenium ion intermediates at nearby sites reduces TS mobility, leading to a higher rate of carbenium ion deprotonation and the donation of protons to the zeolite with a greater density of active sites.

Based on an understanding of reaction intermediates, process parameters and the topology of the heterogeneous catalyst, numerous challenges related to the location and distribution of active sites can be explored to improve selectivity and catalytic activity. For instance, Murphy and collaborators (Murphy et al., 2015; Murphy et al., 2019; Wu et al., 2019), used in situ FTIR to extensively investigate the formation of extrinsic BAS on Na-Y. The researchers showed that the catalytic properties of BAS in Na-Y not only differ from the intrinsic BAS in proton-exchanged FAU, but also depend on the precursor molecule. Stronger acids can be able to dissociatively displace weaker acids adsorbed on Na-Y, favoring the replacement of weaker acid sites with stronger acid sites in the structure.

Other acidic catalysts, such as metal-organic frameworks (MOFs), are considered ideal platforms for the synthesis of organic compounds due to the infinite design possibilities (Bavykina et al., 2020; Wei et al., 2020). Recently Villoria-del-Alamo et al. (2020) studied the amide esterification catalyzed by zirconia-based MOFs (Zr-MOF-808-P), and proposed a plausible mechanism using in situ FTIR (Fig. 8) (Villoria-del-Álamo et al., 2020).

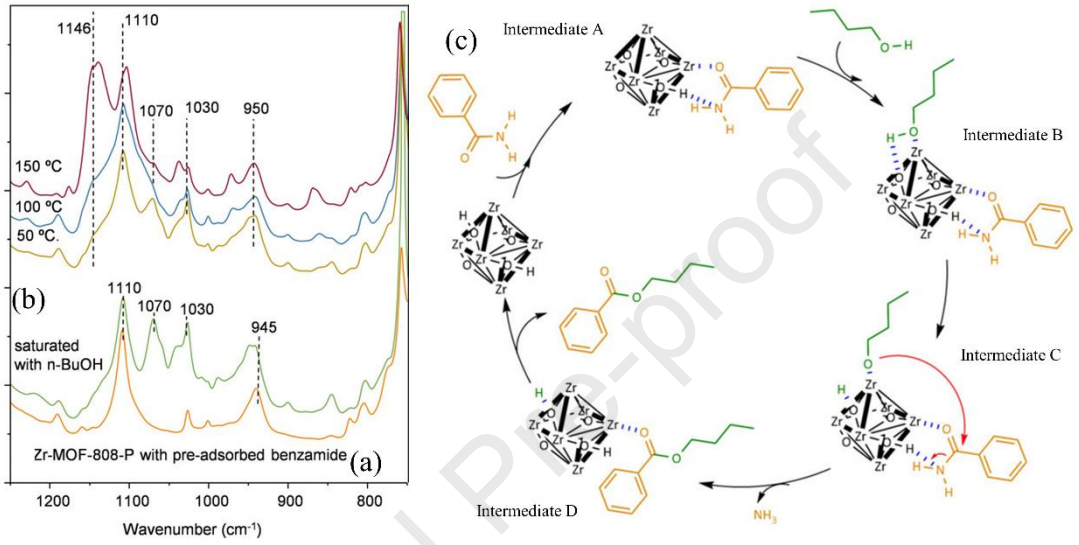

Fig. 8. FTIR spectra in 1250–750 cm^{-1} range of a) Zr-MOF-808-P with pre-adsorbed benzamide, b) Zr-MOF-808-P with pre-absorbed benzamide saturated with *n*-BuOH at room temperature. The temperature was increased for the latter sample at 50 °C, 100 °C and 150 °C and FTIR spectra recorded and shown at the top of the graphic. (c) Proposal mechanism for the benzamide esterification with *n*-BuOH catalyzed by Zr-MOF-808-P, from Villoria-del-Álamo et al. (2020).

The IR spectra (Fig. 8a) indicated the formation of butoxide species at the terminal positions of the catalyst. This is evidenced by a decrease in the centered signal at 1070 cm^{-1} and the appearance of a new band at 1146 cm^{-1}. Subsequently, a mechanism is proposed (Fig. 8 c) based on the spectroscopic results. The authors suggested that both reagents are adsorbed on the surface of the catalyst. However, the intermediate (butoxide) is formed at 150°C and then reacts with the benzamide to form the desired product, releasing NH_3.

Alegre et al. (2019; 2021), using IR spectroscopy with DFT calculations and a theoretical cluster structure model, studied the mechanism for the transesterification of ethyl acetate and methanol at the pore mouth of the [CTA^+]-Si-MCM-41 catalyst. They reported that the experimental FTIR spectrum was

798 supported by the theoretical model for the coadsorption of both reagents following a dual-site mechanism,
799 even though the electronic properties of the catalytic system were explored through electrostatic potential
800 maps.

801 Many reactions involving the conversion biomass occur in the liquid phase, requiring careful
802 consideration of the structure-activity relationship due to the multiple interactions at the solid-liquid
803 interface (Negahdar et al., 2020). Therefore, the effect of water molecules on the heterogeneous catalytic
804 conversion of olefins and MeOH to aromatics on H-ZSM-5 was studied using in situ FTIR spectroscopy,
805 TG, GC-SM, and computational calculations (Wang et al., 2020). The combination of experimental and
806 theoretical techniques showed that the presence of water reduces the conversion of ethylene into aromatics
807 during reactions at temperatures ≤ 300°C. This hindrance is due to the preferential adsorption of water on
808 the BAS, which favors the formation of hydronium ions. The latter decreases the concentration of reactive
809 intermediates adsorbed on the active sites. Similar results for the dehydration of cyclohexanol in the liquid
810 phase on H-BEA through molecular dynamics simulations showed that clusters of water molecules inside
811 zeolite pores affect the reaction mechanism, resulting in decreased the catalytic activity (Mei and Lercher,
812 2019).

813 It has been shown that DFT level electronic structure calculations are commonly used to complement
814 IR spectroscopy data, allowing the identification of bands that are difficult to analyze experimentally with
815 high precision. Manookian et al. (2020) demonstrated the combination of DRIFT spectroscopy and DFT
816 calculations on olefins adsorbed on protonated zeolites and on porous silicas, investigating different
817 rotational conformations of olefin (2,4-dimethyl-1,3-pentadiene) (Fig. 9). They discovered that, the s-cis
818 gauche conformation is more favorable than the s-trans conformation in dealuminated zeolite β. On the
819 other hand, in protonated zeolites (H-MOR), the spectrum changes as result of protonated species (singlet,
820 1500-1600 cm^{-1}), although the analysis of structures suggests that the electrostatic interactions of ion pairs
821 have a negligible effect on these cations in zeolites. These results highlight that experimental and theoretical
822 studies with high precision can be used to elucidate complex intermediates in zeolite systems.

823 More recently, the combination of FTIR spectroscopy, solid-state NMR, and DFT calculations has been
824 used to explore the different types of hydroxyl groups present on the outer surface of ZSM-5 (Treps et al.,
825 2021). Notably, it was possible to correlate the data attributed to the observed experimental resonance
826 through theoretical calculations. The complementarity of the experimental techniques enabled the
827 separation of overlapping signals and the identification of other O-H groups on the catalyst surface. Many

studies have demonstrated the successful combination of NMR and IR applied in the characterization and application of various catalytic systems have been successfully demonstrated (Paul et al., 2018).

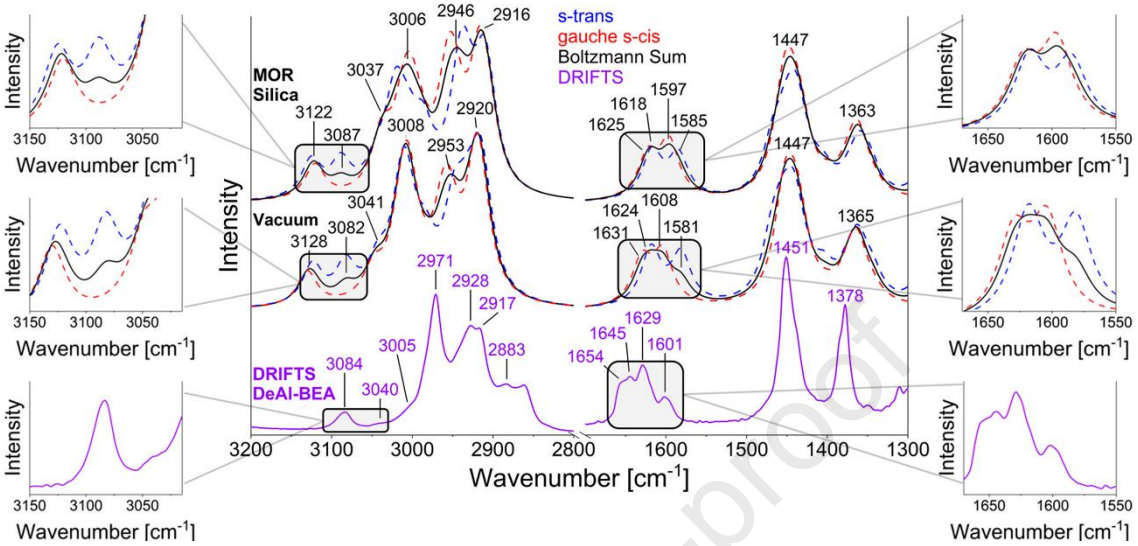

Fig. 9. Comparison of computed and experimental spectra of molecule I. DRIFT spectrum (purple) was taken at 20 °C over Al-BEA. Computed spectra for molecules I in all-silica MOR (top) and in gas phase (middle). In each environment, the spectrum associated with s-trans (blue), gauche s-cis (red), and the Boltzmann sum (black) are shown. Wavenumber values apply to Boltzmann sum. Side panels focus on (left) high-frequency (C–H stretch) and (right) low-frequency (C=C stretch) regions, from Manookian et al (2020).

4. 1. IR spectrum strategies dedicated to the search for intermediates

In order to optimize strategies for the synthesis of new heterogeneous catalysts, it is crucial to understand the relationship between the reaction cycle and the catalyst topology. However, the diversity of species observed in the phenomena of adsorption, product formation, and desorption phenomena suggests spectral overlap as these are processes that occur simultaneously, making it impossible to identify the actual species present in the reaction medium, which constitute elementary steps of a particular reaction mechanism. Spectroscopic techniques combined with sophisticated treatments can extract significant information from the reactions of the solid surface. Thus, the combination of modulation excitation spectroscopy (MES) and phase sensitive detection (PSD) yields significantly enhanced sensitivity for identifying active and spectator species involved in the studied process, and effectively eliminates noise interference (Marchionni et al., 2017)

In experiments involving MES, an external parameter (temperature, concentration, pH, pressure, electric field, radiation, etc.) is perturbed, stimulating the system around the steady state while time-resolved data are simultaneously collected. This approach allows all active species throughout the experiment to change periodically at the same frequency as the external stimulus. However, with a phase delay, this change can carry with it the kinetic constant of a given elementary reaction step. Consequently, the tracking of the reaction provides data on the real-time operando conditions of the catalyst.

The results observed through MES need to be optimized for the detection of sensitive species and the removal of the noise effect present over time. In this sense, Baurecht and Fringeli (2001), based on vectors, developed the PSD method, which enables the demodulation after the acquisition of time-resolved spectra. This mathematical treatment transforms the time domain into the phase domain of the average spectra, as shown in Eq. 5 and Fig. 10.

$$A_k(\Phi_k^{PSD}) = \frac{2}{T}\int_0^T A(t)\,\sin\left(k\omega t + \Phi_k^{PSD}\right)\,dt \quad (5)$$

Where $A_k(\Phi_k^{PSD})$ is the response of the active species in the phase domain*; T* is the length referring to the period; $A(t)$ is the response of the active species in the time domain multiplied by a Sen function; parameter k determines the demodulation index; ω is the external stimulus frequency; Φ_k^{PSD} is the demodulation phase angle. Thus, Eq. 5 shows that only the species that follow the fundamental frequency ω are observed in the phase domain, as shown in Fig. 10. In addition, the signal-to-noise ratio is improved since the noise frequency is higher than the frequency of the active species. Nevertheless, a detailed analysis of $A_k\left(\Phi_k^{PSD}\right)$, allows us to investigate the absolute phase delay φ which, unlike transient experiments resolved in time, is well defined.

The application of the MES-PSD approach to catalytic processes can extend to diverse spectroscopic techniques (Ferri et al., 2010; Müller and Hermans, 2017; Srinivasan et al., 2019; Hess, 2021; Redekop et al., 2021). However, appropriate conditions during the experiment are necessary, such as: (i) the studied reactions must be reversible or pseudo-reversible; (ii) the time resolution of the chosen spectroscopic technique corresponds to the reaction kinetics; (iii) no significant deactivation of the catalyst may occur during the period of a given experiment; and (iv) limitations in mass transport must be avoided in order to obtain accurate information about the kinetics of the process (Müller and Hermans, 2017).

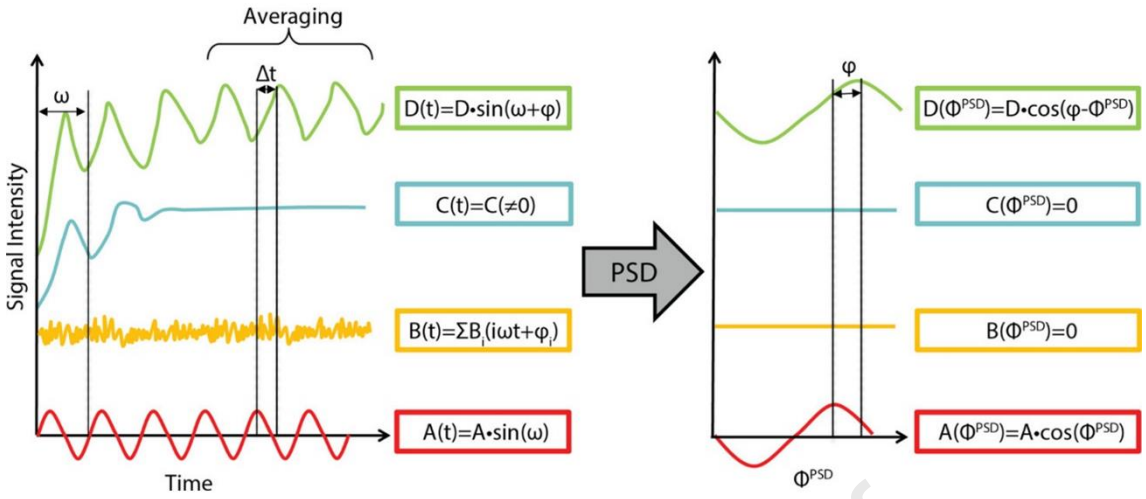

Fig. 10. Illustration of the working principle of PSD. *A*(*t*) is the stimulation function, *B*(*t*) is noise, *C*(*t*) is a response of a spectator species, and *D*(*t*) is the response of an active species. The stimulation function is, in this case, a sine wave with frequency ω. Demodulation using PSD transforms time-domain spectra to the phase domain. Instead of being time-dependent, the spectra are now a function of the phase angle Φ_{PSD}. Instead of appearing at a certain time delay Δ*t*, in the phase domain, the absolute phase delay φ contains information about the dynamics and kinetics of the studied system, from Müller and Hermans (2017).

To exemplify the practicality of IR spectroscopy in the analysis of diverse catalytic systems using MES-PSD, numerous investigations have utilized this technique to explore both metal oxides (Alcaraz et al., 2019; Aguirre and Collins, 2020; Aguirre et al., 2022; Vecchietti et al., 2023) and zeolites (Abdul Nasir et al., 2023; Sun et al., 2023) and recently in biocatalysis with the Novozym® 435 (Toledo et al., 2021). In this sense, liquid phase investigations utilizing ATR spectroscopy with MES-PSD indicate that this approach, when coupled with proper instrumentation, produces excellent results with high precision (Bürgi and Baiker, 2006; Andanson and Baiker, 2010; Aguirre et al., 2011; Müller and Hermans, 2017; Toledo et al., 2017; Chen et al., 2018). Furthermore, The integration of chemometric methods, such as multivariate curve resolution-alternating least squares (MCR-ALS), into the MES-PSD enhances its analytical capabilities by facilitating the extraction of significant spectral and kinetic data from active species (Alcaraz et al., 2019). Therefore, these methodology has the potential to elucidate the various mechanistic proposals for esterification and provide a new perspective on the effect of confined voids when combined with electronic structure calculations.

However, due to the lack of available instrumentation and the numerical method's complexity required to implement the PSD methodology (Srinivasan et al., 2019), to the best of our knowledge, this technique

has not been applied to esterification catalyzed by acid zeolites. The main reason is the difficult control of variables (temperature, pressure, reagent concentration, catalyst properties, type of solvent used during the reaction, among others) that affect the kinetic processes in the condensed phase. This results in the absence or overlapping of bands that inhibit the identification of possible intermediates.

Therefore, due to the potential of these technique, there is a clear need to expand and improve this methodology for research aimed at the valorization of renewable raw materials such as FFA, as well as to study the role of bystander species in the aqueous phase in the deactivation of zeolitic catalysts. These observations, when combined with quantum chemical calculations, will improve the molecular understanding of the conversion of oleaginous residues and provide greater added value to the catalytic processes existing in the chemical industry. Furthermore, the effect of water on reaction mechanisms and rates should be increasingly incorporated into modeling techniques to explore key steps under real reaction conditions (Van Speybroeck et al., 2023).

Finally, previous research has mainly used kinetic data to explore the esterification mechanism in various zeolite systems. This review shows that quantum computational calculations can enhance the understanding and characterization of both the zeolite catalysts and the adsorbed species. The cases presented in this review serve to underline the significance of using in situ and operando IR spectroscopy in combination with quantum calculations for the study of various dynamic processes. It has been shown that the use of advanced IR spectroscopy techniques, such as MES-PSD, allows the identification of species involved in reaction mechanisms under operating conditions. The application of these techniques, in combination with theoretical calculations, leads to highly accurate results. Hence, the synergy between experimental and theoretical studies is essential to improve the understanding of the esterification reaction in zeolite systems.

From a reaction point of view, the esterification of carboxylic acids catalyzed by acidic zeolites presents some of the challenges identified in this review. First, zeolite catalysts are highly sensitive to water (even in small amounts). This requires effective methods to remove or prevent water from the reaction mixture. Second, these materials undergo structural changes and lose their acidity over time due to exposure to high temperatures and adsorbed reactive species. Third, achieving high reaction and conversion rates while maintaining selectivity is a topic that has yet to be explored in the literature. However, the mechanistic information obtained by experimental methods in conjunction with computer modeling and simulations can guide the synthesis of new materials, predict the affinity between organic structure and topology directing

933 agents (Schwalbe-Koda et al., 2021; Schwalbe-Koda and Gómez-Bombarelli, 2023), guide catalyst
934 optimization, and open new perspectives for more sustainable and efficient esterification processes.
935
936 **5. Conclusions, knowledge gaps, and perspectives**
937 Acidic zeolites are highly active in the esterification reaction and can act as excellent remediation
938 materials in the valorization of FFA`s. In this review, we discuss different proposals for esterification
939 mechanisms on acidic zeolites emphasizing the role of IR spectroscopy experiments and theoretical
940 calculations in providing novel insights into the nature of the interactions of intermediates in confined voids.
941 The catalytic performance of different zeolite types for liquid phase esterification is influenced by their
942 physicochemical properties, including hydrophobicity, extra framework Al, specific area, and porosity. The
943 presence of water contributes to the low conversions observed in some esterification reactions due to
944 adsorption on the active sites. In this case, zeolites with a high Si/Al ratio can overcome these effects due
945 to the greater distribution and accessibility of active sites, contributing to the greater stability and durability
946 of these materials during the esterification process. Furthermore, different kinetic models for esterification
947 proved to have an excellent fit with experimental data, however only the L-H and E-R models have
948 excellent parameterizations to describe the adsorption mechanism. Although there are several discussion
949 on the elementary steps of the esterification mechanism in confined environments, it is recognized that the
950 adsorption step is most likely due to the H_Z sharing between an alcohol molecule and a carboxylic acid,
951 resulting in the formation of an energetically stable adsorption complex. This has been demonstrated by
952 studies using DFT calculations.
953 To understand the esterification of carboxylic acids over zeolites, the use of spatial and temporal
954 resolution infrared spectroscopy strategies, both in situ and operando, proves to be highly effective for
955 reaction mechanism studies through MES-PSD in heterogeneous catalysis. This approach yields excellent
956 results in the detection of short-lived intermediates, often overlooked due to the overlap of bands from
957 spectator species. However, despite its great potential, this technique has not yet been reported for the
958 esterification of carboxylic acids using acid zeolites as catalysts. The reason for this is the need for tight
959 control over various variables (temperature, pressure, reactant concentration, catalyst properties, type of
960 solvent used during the reaction, among others) that influence the kinetic processes in the condensed phase.
961 The processes involving acidic zeolites in the petrochemical industry are similar to the conversion
962 processes of oleaginous biomass, which leads us to believe that the fundamental concepts about the

963 topology of the different zeolitic structures can be applied to the esterification reaction. Although there is a
964 discussion about the elementary steps of the esterification mechanism in confined environments, it is
965 recognized that there are gaps to be investigated:

966 *(I)* The esterification reaction takes place preferably in a liquid medium, therefore, exploring
967 characterizations in reaction conditions will allow a better understanding of the activity of acidic sites
968 (BAS/LAS) and the confinement effect caused within the pores and cavities of different systems zeolites.
969 Furthermore, the use of MES-PSD methods applied in IR spectroscopy will allow enable a more detailed
970 analysis of the esterification mechanism, contributing to the optimization of the efficiency of zeolitic
971 catalysts in this context.

972 *(II)* Most of the studies on the esterification reaction catalyzed by zeolites have been carried out under
973 batch conditions. However, to enable the applicability of these catalysts in industrial processes for the
974 conversion of FFA's, continuous flow systems need to be explored in order to favor an economically viable
975 process.

976 *(III)* Computational calculations should gain space in future studies, because they can contribute to the
977 determination of reaction mechanisms in heterogeneous catalysis, to the prediction of reaction parameters,
978 and provide researchers with data for the rationalization of experimental observations, up to the point of
979 optimizing the more sustainable synthesis of new zeolitic materials. An approach that integrates
980 experimentation and computational modeling, can significantly accelerate the development of the
981 understanding of the esterification reaction on acidic zeolites with improved catalytic properties, thus
982 contributing to innovative advances in the valorization of FFA's.

983 An in-depth understanding of acid zeolite catalysis at the molecular level is crucial for boosting the
984 process on an industrial scale and, ultimately, aiding the advancement of future applications. This review
985 provides an invaluable and widely relevant resource to inform and highlight new research dedicated to
986 exploring the application of acidic zeolites in the transformation of different oilseed biomass. Our work on
987 the combination of experimental and theoretical techniques in esterification catalyzed by acidic zeolites is
988 still in progress, and will certainly shed light on the reaction mechanism at both the molecular and the
989 experimental levels.

990

991 **Acknowledgements:** This research was made possible by Consejo Nacional de Investigaciones Científicas
992 y Técnicas (CONICET) and Secretaría General de Ciencia y Técnica of the Universidad Nacional del

Nordeste (SGCyT-UNNE) of Argentine. The Fundação Araucária, the Coordenação de Aperfeiçoamento de Pessoal de Nível Superior (CAPES), the Conselho Nacional de Desenvolvimento Científico e Tecnológico (CNPq), and the Fundação Parque Tecnológico Itaipu (FPTI), for the support received.

Reference

Abdul Nasir, J., Guan, J., Keal, T.W., Desmoutier, A.W., Lu, Y., Beale, A.M., Catlow, C.R.A., Sokol, A.A., 2023. Influence of Solvent on Selective Catalytic Reduction of Nitrogen Oxides with Ammonia over Cu-CHA Zeolite. J. Am. Chem. Soc. 145, 247-259.

Aguirre, A., Bonivardi, A.L., Matkovic, S.R., Briand, L.E., Collins, S.E., 2011. ATR-FTIR Study of the Decomposition of Acetic Anhydride on Fosfotungstic Wells–Dawson Heteropoly Acid Using Concentration-Modulation Excitation Spectroscopy. Top, Catal. 54, 229-235.

Aguirre, A., Collins, S.E., 2020. Design of an optimized DRIFT cell/microreactor for spectrokinetic investigations of surface reaction mechanisms. Mol. Catal. 481, 100628.

Aguirre, A., Fornero, E.L., Villarreal, A., Collins, S.E., 2022. Identification of key reaction intermediates during toluene combustion on a Pd/CeO2 catalyst using operando modulated DRIFT spectroscopy. Catal. Today 394-396, 225-234.

Ahmed, R., Huddersman, K., 2022. Review of biodiesel production by the esterification of wastewater containing fats oils and grease (FOGs). J. Ind. Eng. Chem. 110, 1-14.

Alaba, P.A., Sani, Y.M., Mohammed, I.Y., Daud, W.M.A.W., 2016. Insight into catalyst deactivation mechanism and suppression techniques in thermocatalytic deoxygenation of bio-oil over zeolites. Rev. Chem. Eng. 32, 71-91.

Alcaraz, M.R., Aguirre, A., Goicoechea, H.C., Culzoni, M.J., Collins, S.E., 2019. Resolution of intermediate surface species by combining modulated infrared spectroscopy and chemometrics. Anal. Chim. Acta 1049, 38-46.

Alegre, C.I.A., Cazula, B.B., Alves, H.J., Zalazar, M.F., Peruchena, N.M., 2021. The key role of adsorbate-catalyst interactions into catalytic activity of [CTA+]-Si-MCM-41 from electron density analysis. Mol. Catal. 504, 111472.

1021 Alegre, C.I.A., Zalazar, M.F., Bulhões Cazula, B., Alves, H.J., Peruchena, N.M., 2019. Molecular Insights
1022 on the Role of (CTA+)(SiO−) Ion Pair into the Catalytic Activity of [CTA+]–Si–MCM-41. Top. Catal. 62,
1023 941-955.

1024 Andanson, J.-M., Baiker, A., 2010. Exploring catalytic solid/liquid interfaces by in situ attenuated total
1025 reflection infrared spectroscopy. Chem. Soc. Rev. 39, 4571-4584.

1026 Aranda, D.A.G., Gonçalves, J.d.A., Peres, J.S., Ramos, A.L.D., de Melo, C.A.R., Antunes, O.A.C., Furtado,
1027 N.C., Taft, C.A., 2009. The use of acids, niobium oxide, and zeolite catalysts for esterification reactions. J.
1028 Phys. Org.Chem. 22, 709-716.

1029 Arca, H.A., Gomes, G.C.C., Mota, C.J.A., 2014. Solid solvents: activation parameters for the rearrangement
1030 of cyclopropylcarbinyl bromide on mordenite zeolite. New J. Chem. 38, 2760-2762.

1031 Arca, H.A., Mota, C.J.A., 2018. Rearrangement of Cyclopropylcarbinyl Chloride Over Protonic Zeolites:
1032 Formation of Carbocations and Behavior as Solid Solvents. Top. Catal. 61, 616-622.

1033 Atadashi, I.M., Aroua, M.K., Abdul Aziz, A.R., Sulaiman, N.M.N., 2013. The effects of catalysts in
1034 biodiesel production: A review. J. Ind. Eng. Chem 19, 14-26.

1035 Atzori, C., Lomachenko, K.A., Jacobsen, J., Stock, N., Damin, A., Bonino, F., Bordiga, S., 2020. Bimetallic
1036 hexanuclear clusters in Ce/Zr-UiO-66 MOFs: in situ FTIR spectroscopy and modelling insights. Dalton T.
1037 49, 5794-5797.

1038 Bai, R., Song, Y., Li, Y., Yu, J., 2019. Creating Hierarchical Pores in Zeolite Catalysts. Trends Chem. 1,
1039 601-611.

1040 Baurecht, D., Fringeli, U.P., 2001. Quantitative modulated excitation Fourier transform infrared
1041 spectroscopy. Rev. Sci. Instrum. 72, 3782-3792.

1042 Bavykina, A., Kolobov, N., Khan, I.S., Bau, J.A., Ramirez, A., Gascon, J., 2020. Metal–Organic
1043 Frameworks in Heterogeneous Catalysis: Recent Progress, New Trends, and Future Perspectives. Chem.
1044 Rev. 120, 8468-8535.

1045 Bedard, J., Chiang, H., Bhan, A., 2012. Kinetics and mechanism of acetic acid esterification with ethanol
1046 on zeolites. J. Catal. 290, 210-219.

1047 Ben Mya, O., Bita, M., Louafi, I., Djouadi, A., 2018. Esterification process catalyzed by ZSM-5 zeolite
1048 synthesized via modified hydrothermal method. MethodsX 5, 277-282.

1049 Bertella, F., Lopes, C.W., Foucher, A.C., Agostini, G., Concepción, P., Stach, E.A., Martínez, A., 2020.
1050 Insights into the Promotion with Ru of Co/TiO2 Fischer–Tropsch Catalysts: An In Situ Spectroscopic
1051 Study. ACS Catal. 10, 6042-6057.

1052 Bocus, M., Neale, S.E., Cnudde, P., Van Speybroeck, V., 2021. Dynamic evolution of catalytic active sites
1053 within zeolite catalysis. Reference Module in Chemistry, Molecular Sciences and Chemical Engineering.
1054 Elsevier.

1055 Bordiga, S., Lamberti, C., Bonino, F., Travert, A., Thibault-Starzyk, F., 2015. Probing zeolites by
1056 vibrational spectroscopies. Chem. Soc. Rev. 44, 7262-7341.

1057 Boronat, M., Climent, M.J., Concepción, P., Díaz, U., García, H., Iborra, S., Leyva-Pérez, A., Liu, L.,
1058 Martínez, A., Martínez, C., Moliner, M., Pérez-Pariente, J., Rey, F., Sastre, E., Serna, P., Valencia, S., 2022.
1059 A Career in Catalysis: Avelino Corma. ACS Catal. 12, 7054-7123.

1060 Boronat, M., Corma, A., 2015. Factors Controlling the Acidity of Zeolites. Catal. Lett. 145, 162-172.

1061 Boronat, M., Corma, A., 2019. What Is Measured When Measuring Acidity in Zeolites with Probe
1062 Molecules? ACS Catal. 9, 1539-1548.

1063 Bürgi, T., Baiker, A., 2006. Attenuated Total Reflection Infrared Spectroscopy of Solid Catalysts
1064 Functioning in the Presence of Liquid-Phase Reactants. in: Gates, B.C., Knzinger, H. (Eds.). Advances in
1065 Catalysis. Academic Press, pp. 227-283.

1066 Cabrera-Munguia, D.A., González, H., Gutiérrez-Alejandre, A., Rico, J.L., Huirache-Acuña, R., Maya-
1067 Yescas, R., del Río, R.E., 2017. Heterogeneous acid conversion of a tricaprylin-palmitic acid mixture over
1068 Al-SBA-15 catalysts: Reaction study for biodiesel synthesis. Catal. Today 282, 195-203.

1069 Canhaci, S.J., Albuquerque, E.M., Lopes, C.C., Faria, V.W., Chinelatto Junior, L.S., Duarte de Farias,
1070 A.M., Quitete, C.B., Fraga, M.A., 2023. Balance between Catalyst Acidity and Hydrophilicity in Biofuel
1071 Production from Fatty Acid Esterification over Al-SBA-15. Catalysts 13, 827.

1072 Chaemchuen, S., Heynderickx, P.M., Verpoort, F., 2020. Kinetic modeling of oleic acid esterification with
1073 UiO-66: from intrinsic experimental data to kinetics via elementary reaction steps. Chem. Eng. J. 394,
1074 124816.

1075 Chen, B.W.J., Xu, L., Mavrikakis, M., 2021. Computational Methods in Heterogeneous Catalysis. Chem.
1076 Rev. 121, 1007-1048.

1077 Chen, L.-H., Sun, M.-H., Wang, Z., Yang, W., Xie, Z., Su, B.-L., 2020. Hierarchically Structured Zeolites:
1078 From Design to Application. Chem. Rev. 120, 11194-11294.

1079 Chen, M., Maeda, N., Baiker, A., Huang, J., 2018. Hydrogenation of Acetophenone on Pd/Silica–Alumina
1080 Catalysts with Tunable Acidity: Mechanistic Insight by In Situ ATR-IR Spectroscopy. ACS Catal. 8, 6594-
1081 6600.

1082 Chen, W., Tarach, K.A., Yi, X., Liu, Z., Tang, X., Góra-Marek, K., Zheng, A., 2022. Charge-separation
1083 driven mechanism via acylium ion intermediate migration during catalytic carbonylation in mordenite
1084 zeolite. Nat. Commun. 13, 7106.

1085 Chouhan, A.P.S., Sarma, A.K., 2011. Modern heterogeneous catalysts for biodiesel production: A
1086 comprehensive review. Renew. Sust. Energ. Rev. 15, 4378-4399.

1087 Chung, K.-H., Chang, D.-R., Park, B.-G., 2008. Removal of free fatty acid in waste frying oil by
1088 esterification with methanol on zeolite catalysts. Bioresource Technol. 99, 7438-7443.

1089 Chung, K.-H., Park, B.-G., 2009. Esterification of oleic acid in soybean oil on zeolite catalysts with different
1090 acidity. J. Ind. Eng. Chem. 15, 388-392.

1091 Ciddor, L., Bennett, J.A., Hunns, J.A., Wilson, K., Lee, A.F., 2015. Catalytic upgrading of bio-oils by
1092 esterification. J. Chem. Technol. Biot. 90, 780-795.

1093 Corma, A., 1995. Inorganic Solid Acids and their Use in Acid-Catalyzed Hydrocarbon Reactions. Chem.
1094 Rev. 95, 559–614.

1095 Corma, A., 1997. From Microporous to Mesoporous Molecular Sieve Materials and Their Use in Catalysis.
1096 Chem. Rev. 97, 2373-2420.

1097 Corma, A., 2003. State of the art and future challenges of zeolites as catalysts. J. Catal. 216, 298-312.

1098 Corma, A., 2016. Heterogeneous Catalysis: Understanding for Designing, and Designing for Applications.
1099 Angew. Chem., Int. Ed. 55, 6112-6113.

1100 Corma, A., Garcia, H., Iborra, S., Primo, J., 1989. Modified faujasite zeolites as catalysts in organic
1101 reactions: Esterification of carboxylic acids in the presence of HY zeolites. J. Catal. 120, 78-87.

1102 Costa, R.J., Castro, E.A.S., Politi, J.R.S., Gargano, R., Martins, J.B.L., 2019. Methanol, ethanol, propanol,
1103 and butanol adsorption on H-ZSM-5 zeolite: an ONIOM study. J. Mol. Model. 25, 34.

Creci, S., Martinelli, A., Vavra, S., Carlsson, P.-A., Skoglundh, M., 2021. Acidity as Descriptor for Methanol Desorption in B-, Ga- and Ti-MFI Zeotypes. Catalysts 11, 97.

Dabros, T.M.H., Stummann, M.Z., Høj, M., Jensen, P.A., Grunwaldt, J.-D., Gabrielsen, J., Mortensen, P.M., Jensen, A.D., 2018. Transportation fuels from biomass fast pyrolysis, catalytic hydrodeoxygenation, and catalytic fast hydropyrolysis. Prog. Energ. Combust. Sci. 68, 268-309.

Dal Pozzo, D.M., Azevedo dos Santos, J.A., Júnior, E.S., Santos, R.F., Feiden, A., Melegari de Souza, S.N., Burgardt, I., 2019. Free fatty acids esterification catalyzed by acid Faujasite type zeolite. RSC Adv. 9, 4900-4907.

del Campo, P., Martínez, C., Corma, A., 2021. Activation and conversion of alkanes in the confined space of zeolite-type materials. Chem. Soc. Rev. 50,8511-8595.

Derouane, E.G., 1986. Shape selectivity in catalysis by zeolites: The nest effect. J. Catal. 100, 541-544.

Derouane, E.G., 1998. Zeolites as solid solvents1Paper presented at the International Symposium `Organic Chemistry and Catalysis' on the occasion of the 65th birthday of Prof. H. van Bekkum, Delft, Netherlands, 2–3 October 1997.1. J. Mol. Catal. A: Chem. 134, 29-45.

Derouane, E.G., Andre, J.-M., Lucas, A.A., 1988. Surface curvature effects in physisorption and catalysis by microporous solids and molecular sieves. J. Catal. 110, 58-73.

Deshlahra, P., Iglesia, E., 2020. Reactivity descriptors in acid catalysis: acid strength, proton affinity and host–guest interactions. Chem. Commun. 56, 7371-7398.

Doyle, A.M., Albayati, T.M., Abbas, A.S., Alismaeel, Z.T., 2016. Biodiesel production by esterification of oleic acid over zeolite Y prepared from kaolin. Renew. Energy 97, 19-23.

Doyle, A.M., Alismaeel, Z.T., Albayati, T.M., Abbas, A.S., 2017. High purity FAU-type zeolite catalysts from shale rock for biodiesel production. Fuel 199, 394-402.

Endalew, A.K., Kiros, Y., Zanzi, R., 2011. Inorganic heterogeneous catalysts for biodiesel production from vegetable oils. Biomass Bioenergy 35, 3787-3809.

Ennaert, T., Van Aelst, J., Dijkmans, J., De Clercq, R., Schutyser, W., Dusselier, M., Verboekend, D., Sels, B.F., 2016. Potential and challenges of zeolite chemistry in the catalytic conversion of biomass. Chem. Soc. Rev. 45, 584-611.

1131 Fattahi, N., Triantafyllidis, K., Luque, R., Ramazani, A., 2019. Zeolite-Based Catalysts: A Valuable
1132 Approach toward Ester Bond Formation. Catalysts 9, 758.

1133 Fawaz, E.G., Salam, D.A., Daou, T.J., 2020. Esterification of linoleic acid using HZSM-5 zeolites with
1134 different Si/Al ratios. Microporous Mesoporous Mater. 294, 109855.

1135 Fawaz, E.G., Salam, D.A., Pinard, L., Daou, T.J., 2019. Study on the catalytic performance of different
1136 crystal morphologies of HZSM-5 zeolites for the production of biodiesel: a strategy to increase catalyst
1137 effectiveness. Catal. Sci. Technol. 9, 5456-5471.

1138 Fawaz, E.G., Salam, D.A., S. Rigolet, S., Daou, T.J., 2021. Hierarchical Zeolites as Catalysts for Biodiesel
1139 Production from Waste Frying Oils to Overcome Mass Transfer Limitations. Molecules 26, 4879.

1140 Fereidooni, L., Enayati, M., Abbaspourrad, A., 2021. Purification technology for renewable production of
1141 fuel from methanolysis of waste sunflower oil in the presence of high silica zeolite beta. Green Chem. Lett.
1142 Rev. 14, 2-14.

1143 Fernandes, D.R., Rocha, A.S., Mai, E.F., Mota, C.J.A., Teixeira da Silva, V., 2012. Levulinic acid
1144 esterification with ethanol to ethyl levulinate production over solid acid catalysts. Appl. Catal., A 425–426,
1145 199-204.

1146 Ferri, D., Kumar, M.S., Wirz, R., Eyssler, A., Korsak, O., Hug, P., Weidenkaff, A., Newton, M.A., 2010.
1147 First steps in combining modulation excitation spectroscopy with synchronous dispersive
1148 EXAFS/DRIFTS/mass spectrometry for in situ time resolved study of heterogeneous catalysts. Phys. Chem.
1149 Chem. Phys. 12, 5634-5646.

1150 Ferri, P., Li, C., Schwalbe-Koda, D., Xie, M., Moliner, M., Gómez-Bombarelli, R., Boronat, M., Corma,
1151 A., 2023. Approaching enzymatic catalysis with zeolites or how to select one reaction mechanism
1152 competing with others. Nat. Commun. 14, 2878.

1153 Fu, J., Feng, X., Liu, Y., Yang, C., 2017. Effect of pore confinement on the adsorption of mono-branched
1154 alkanes of naphtha in ZSM-5 and Y zeolites. Appl. Surf. Sci. 423, 131-138.

1155 Gołąbek, K., Tabor, E., Pashkova, V., Dedecek, J., Tarach, K., Góra-Marek, K., 2020. The proximity of
1156 aluminium atoms influences the reaction pathway of ethanol transformation over zeolite ZSM-5. Commun.
1157 Chem. 3, 25.

Gomes, G.J., Costa, M.B., Bittencourt, P.R.S., Zalazar, M.F., Arroyo, P.A., 2021. Catalytic improvement of biomass conversion: Effect of adding mesoporosity on MOR zeolite for esterification with oleic acid. Renew. Energy. 178, 1-12.

Gomes, G.J., Dal Pozzo, D.M., Zalazar, M.F., Costa, M.B., Arroyo, P.A., Bittencourt, P.R.S., 2019a. Oleic Acid Esterification Catalyzed by Zeolite Y-Model of the Biomass Conversion. Top. Catal. 62, 874–883.

Gomes, G.J., Zalazar, M.F., Arroyo, P.A., 2022. New Insights into the Effect of the Zeolites Framework Topology on the Esterification Reactions: A Comparative Study from Experiments and Theoretical Calculations. Top. Catal. 65, 871–886.

Gomes, G.J., Zalazar, M.F., Arroyo, P.A., Scremin, F.R., Costa, M.B., Bittencourt, P.R.S., Lindino, C.A., Peruchena, N.M., 2019b. Molecular-level Understanding of the Rate-determining Step in Esterification Reactions Catalyzed by H-ZSM-5 Zeolite. An Experimental and Theoretical Study. ChemistrySelect 4, 3031-3041.

Gomes, G.J., Zalazar, M.F., Lindino, C.A., Scremin, F.R., Bittencourt, P.R.S., Costa, M.B., Peruchena, N.M., 2017. Adsorption of acetic acid and methanol on H-Beta zeolite: An experimental and theoretical study. Microporous Mesoporous Mater. 252, 17-28.

Gong, X., Çağlayan, M., Ye, Y., Liu, K., Gascon, J., Dutta Chowdhury, A., 2022. First-Generation Organic Reaction Intermediates in Zeolite Chemistry and Catalysis. Chem. Rev. 122, 14275-14345.

Gorte, R.J., White, D., 1997. Interactions of chemical species with acid sites in zeolites. Top. Catal. 4, 57-69.

Gounder, R., Iglesia, E., 2013. The catalytic diversity of zeolites: confinement and solvation effects within voids of molecular dimensions. Chem. Commun. 49, 3491-3509.

Gupta, P., Paul, S., 2014. Solid acids: Green alternatives for acid catalysis. Catal. Today 236, 153-170.

Han, F., Yuan, M., Chen, H., 2020. Selective catalytic reduction of NOx with methanol on H-ZSM-5: The effect of extra-framework aluminum. Catal. Today 355, 443-449.

Hartmann, M., Machoke, A.G., Schwieger, W., 2016. Catalytic test reactions for the evaluation of hierarchical zeolites. Chem. Soc. Rev. 45, 3313-3330.

Hashemizadeh, A., Bui, Q., Kongbuamai, N., 2021. Unpacking the role of public debt in renewable energy consumption: New insights from the emerging countries. Energy 224, 120187.

1186 Hess, C., 2021. New advances in using Raman spectroscopy for the characterization of catalysts and
1187 catalytic reactions. Chem. Soc. Rev. 50, 3519-3564.

1188 Heynderickx, P.M., Chaemchuen, S., Verpoort, F., 2020. Kinetic modeling of heterogeneous esterification
1189 reaction using initial reaction rate analysis: data extraction and evaluation of mass transfer criteria. Data
1190 Br. 31, 106027.

1191 Hoffman, A.J., Bates, J.S., Di Iorio, J.R., Nystrom, S.V., Nimlos, C.T., Gounder, R., Hibbitts, D., 2020.
1192 Rigid Arrangements of Ionic Charge in Zeolite Frameworks Conferred by Specific Aluminum Distributions
1193 Preferentially Stabilize Alkanol Dehydration Transition States. Angew. Chem. Int. Ed. 59, 18686-18694.

1194 Isernia, L.F., 2014. Study of the influence of physical–chemical properties of steamed H-MOR zeolites in
1195 the mechanism of adsorption of fatty acids and their esterification. Microporous Mesoporous Mater. 200,
1196 19-26.

1197 Jamil, M.A.R., Touchy, A.S., Poly, S.S., Rashed, M.N., Siddiki, S.M.A.H., Toyao, T., Maeno, Z., Shimizu,
1198 K.-i., 2020. High-silica Hβ zeolite catalyzed methanolysis of triglycerides to form fatty acid methyl esters
1199 (FAMEs). Fuel Process. Technol. 197, 106204.

1200 Jermy, B.R., Pandurangan, A., 2005. Catalytic application of Al-MCM-41 in the esterification of acetic
1201 acid with various alcohols. Appl. Catal. A Gen. 288, 25-33.

1202 Jia, X., Khan, W., Wu, Z., Choi, J., Yip, A.C.K., 2019. Modern synthesis strategies for hierarchical zeolites:
1203 Bottom-up versus top-down strategies. Adv. Powder Technol. 30, 467-484.

1204 Jones, A.J., Carr, R.T., Zones, S.I., Iglesia, E., 2014. Acid strength and solvation in catalysis by MFI zeolites
1205 and effects of the identity, concentration and location of framework heteroatoms. J. Catal. 312, 58-68.

1206 Kerstens, D., Smeyers, B., Van Waeyenberg, J., Zhang, Q., Yu, J., Sels, B.F., 2020. State of the Art and
1207 Perspectives of Hierarchical Zeolites: Practical Overview of Synthesis Methods and Use in Catalysis. Adv.
1208 Mater. 32, 2004690.

1209 Ketzer, F., Celante, D., de Castilhos, F., 2020. Catalytic performance and ultrasonic-assisted impregnation
1210 effects on WO3/USY zeolites in esterification of oleic acid with methyl acetate. Microporous Mesoporous
1211 Mater. 291, 109704.

1212 Ketzer, F., de Castilhos, F., 2021. An assessment on kinetic modeling of esterification reaction from oleic
1213 acid and methyl acetate over USY zeolite. Microporous Mesoporous Mater. 314, 110890.

Khalili, K.N.M., de Peinder, P., Bruijnincx, P.C.A., Weckhuysen, B.M., 2021. Monitoring Aqueous Phase Reactions by Operando ATR-IR Spectroscopy at High Temperature and Pressure: A Biomass Conversion Showcase. Chemistry–Methods 1, 468-476.

Khan, A., Chenggang, Y., Hussain, J., Kui, Z., 2021a. Impact of technological innovation, financial development and foreign direct investment on renewable energy, non-renewable energy and the environment in belt & Road Initiative countries. Renew. Energ. 171, 479-491.

Khan, Z., Javed, F., Shamair, Z., Hafeez, A., Fazal, T., Aslam, A., Zimmerman, W.B., Rehman, F., 2021b. Current developments in esterification reaction: A review on process and parameters. J. Ind. Eng. Chem. 103, 80-101.

Kirumakki, S.R., Nagaraju, N., Chary, K.V.R., 2006. Esterification of alcohols with acetic acid over zeolites Hβ, HY and HZSM5. Appl. Catal. A Gen. 299, 185-192.

Kirumakki, S.R., Nagaraju, N., Narayanan, S., 2004. A comparative esterification of benzyl alcohol with acetic acid over zeolites Hβ, HY and HZSM5. Appl. Catal. A Gen. 273, 1-9.

Koster, R., van der Linden, B., Poels, E., Bliek, A., 2001. The Mechanism of the Gas-Phase Esterification of Acetic Acid and Ethanol over MCM-41. J. Catal. 204, 333-338.

Kubička, D., Kikhtyanin, O., 2015. Opportunities for zeolites in biomass upgrading—Lessons from the refining and petrochemical industry. Catal. Today 243, 10-22.

Lakiss, L., Vicente, A., Gilson, J.-P., Valtchev, V., Mintova, S., Vimont, A., Bedard, R., Abdo, S., Bricker, J., 2020. Probing the Brønsted Acidity of the External Surface of Faujasite-Type Zeolites. ChemPhysChem 21, 1873-1881.

Lam, M.K., Lee, K.T., Mohamed, A.R., 2010. Homogeneous, heterogeneous and enzymatic catalysis for transesterification of high free fatty acid oil (waste cooking oil) to biodiesel: A review. Biotechnol. Adv. 28, 500-518.

Lee, A.F., Bennett, J.A., Manayil, J.C., Wilson, K., 2014. Heterogeneous catalysis for sustainable biodiesel production via esterification and transesterification. Chem. Soc. Rev. 43, 7887-7916.

Li, F., Srivatsa, S.C., Bhattacharya, S., 2019. A review on catalytic pyrolysis of microalgae to high-quality bio-oil with low oxygeneous and nitrogenous compounds. Renew. Sust. Energ. Rev. 108, 481-497.

Li, J., Corma, A., Yu, J., 2015. Synthesis of new zeolite structures. Chem. Soc. Rev. 44, 7112-7127.

1242 Li, K., Valla, J., Garcia-Martinez, J., 2014. Realizing the Commercial Potential of Hierarchical Zeolites:
1243 New Opportunities in Catalytic Cracking. ChemCatChem 6, 46-66.

1244 Li, Y., Li, L., Yu, J., 2017. Applications of Zeolites in Sustainable Chemistry. Chem 3, 928-949.

1245 Liang, J., Shan, G., Sun, Y., 2021. Catalytic fast pyrolysis of lignocellulosic biomass: Critical role of zeolite
1246 catalysts. Renew. Sust. Energ. Rev. 139, 110707.

1247 Lilja, J., Murzin, D.Y., Salmi, T., Aumo, J., Mäki-Arvela, P., Sundell, M., 2002. Esterification of different
1248 acids over heterogeneous and homogeneous catalysts and correlation with the Taft equation. J. Mol. Catal.
1249 A Chem. 182-183, 555-563.

1250 Ma, S., Liu, Z.-P., 2022. Machine learning potential era of zeolite simulation. Chem. Sci. 13, 5055-5068.

1251 Manookian, B., Hernandez, E.D., Baer, M.D., Mundy, C.J., Jentoft, F.C., Auerbach, S.M., 2020.
1252 Experimental and DFT Calculated IR Spectra of Guests in Zeolites: Acyclic Olefins and Host–Guest
1253 Interactions. J. Phys. Chem. C 124, 10561-10572.

1254 Marchionni, V., Ferri, D., Kröcher, O., Wokaun, A., 2017. Increasing the Sensitivity to Short-Lived Species
1255 in a Modulated Excitation Experiment. Anal. Chem. 89, 5801-5809.

1256 Martínez–Castelló, A., Tejeda–Serrano, M., Nowacka, A.E., Oliver–Meseguer, J., Leyva–Pérez, A., 2022.
1257 Solid–catalyzed esterification reaction of long–chain acids and alcohols in fixed–bed reactors at pilot plant
1258 scale. Chem. Eng. Process. - Process Intensif. 178, 109038.

1259 Mei, D., Lercher, J.A., 2019. Effects of Local Water Concentrations on Cyclohexanol Dehydration in H-
1260 BEA Zeolites. J. Phys. Chem. C 123, 25255-25266.

1261 Miao, S., Shanks, B.H., 2011. Mechanism of acetic acid esterification over sulfonic acid-functionalized
1262 mesoporous silica. J. Catal. 279, 136-143.

1263 Mitran, G., Chen, S., Dolge, K.L., Huang, W., Seo, D.-K., 2021. Ketonic decarboxylation and esterification
1264 of propionic acid over beta zeolites. Microporous Mesoporous Mater. 310, 110628.

1265 Mowla, O., Kennedy, E., Stockenhuber, M., 2018. In-situ FTIR study on the mechanism of both steps of
1266 zeolite-catalysed hydroesterification reaction in the context of biodiesel manufacturing. Fuel 232, 12-26.
1267 Mowla, O., Kennedy, E., Stockenhuber, M., 2019. Mass transfer and kinetic study on BEA zeolite-catalysed
1268 oil hydroesterification. Renew. Energy 135, 417-425.

Müller, P., Hermans, I., 2017. Applications of Modulation Excitation Spectroscopy in Heterogeneous Catalysis. Ind. Eng. Chem. Res. 56, 1123-1136.

Murphy, B., Davis, M.E., Xu, B., 2015. The Effect of Adsorbed Molecule Gas-Phase Deprotonation Enthalpy on Ion Exchange in Sodium Exchanged Zeolites: An In Situ FTIR Investigation. Top. Catal. 58, 393-404.

Murphy, B.M., Wu, J., Cho, H.J., Soreo, J., Wang, C., Ma, L., Xu, B., 2019. Nature and Catalytic Properties of In-Situ-Generated Brønsted Acid Sites on NaY. ACS Catal. 9, 1931-1942.

Mutlu, V.N., Yilmaz, S., 2016. Esterification of cetyl alcohol with palmitic acid over WO3/Zr-SBA-15 and Zr-SBA-15 catalysts. Appl. Catal. A Gen. 522, 194-200.

Narkhede, N., Patel, A., 2014. Efficient synthesis of biodiesel over a recyclable catalyst comprising a monolacunary silicotungstate and zeolite Hβ. RSC Adv. 4, 64379-64387.

Negahdar, L., Parlett, C.M.A., Isaacs, M.A., Beale, A.M., Wilson, K., Lee, A.F., 2020. Shining light on the solid–liquid interface: in situ/operando monitoring of surface catalysis. Catal. Sci. Technol. 10, 5362-5385.

Nepel, T.C.M., Anchieta, C.G., Cremasco, L.F., Sousa, B.P., Miranda, A.N., Oliveira, L.C.C.B., Francisco, B.A.B., Júlio, J.P.d.O., Maia, F.C.B., Freitas, R.O., Rodella, C.B., Filho, R.M., Doubek, G., 2021. In Situ Infrared Micro and Nanospectroscopy for Discharge Chemical Composition Investigation of Non-Aqueous Lithium–Air Cells. Adv. Energy Mater. 11, 2101884.

Opanasenko, M., 2018. Zeolite constructor kit: Design for catalytic applications. Catal. Today 304, 2-11.

Opanasenko, M., Shamzhy, M., Wang, Y., Yan, W., Nachtigall, P., Čejka, J., 2020. Synthesis and Post-Synthesis Transformation of Germanosilicate Zeolites. Angew. Chem. Int. Ed. 59, 19380-19389.

Ozorio, L.P., Henrique, F.J.S., Comerford, J.W., North, M., Mota, C.J.A., 2021. Zeolite-mediated production of cyclic organic carbonates: reaction of CO2 with styrene oxide on zeolite Y impregnated with metal halides. React. Chem. Eng. 6, 672-678.

Parangi, T., Mishra, M.K., 2020. Solid Acid Catalysts for Biodiesel Production. Comments Inorg. Chem. 40, 176-216.

Patel, A., Brahmkhatri, V., Singh, N., 2013. Biodiesel production by esterification of free fatty acid over sulfated zirconia. Renew. Energy 51, 227-233.

Paul, G., Bisio, C., Braschi, I., Cossi, M., Gatti, G., Gianotti, E., Marchese, L., 2018. Combined solid-state NMR, FT-IR and computational studies on layered and porous materials. Chem. Soc. Rev. 47, 5684-5739.

Peng, Y.-K., Tsang, S.-c.E., 2022. Probe-assisted NMR: Recent progress on the surface study of crystalline metal oxides with various terminated facets. Magn. Reson. Lett. 2, 9-16.

Pérez-Botella, E., Valencia, S., Rey, F., 2022. Zeolites in Adsorption Processes: State of the Art and Future Prospects. Chem. Rev. 122, 17647-17695.

Peters, T.A., Benes, N.E., Holmen, A., Keurentjes, J.T.F., 2006. Comparison of commercial solid acid catalysts for the esterification of acetic acid with butanol. Appl. Catal. A Gen. 297, 182-188.

Piccini, G., Alessio, M., Sauer, J., 2018. Ab initio study of methanol and ethanol adsorption on Brønsted sites in zeolite H-MFI. Phys. Chem. Chem. Phys. 20, 19964-19970.

Prinsen, P., Luque, R., González-Arellano, C., 2018. Zeolite catalyzed palmitic acid esterification. Microporous Mesoporous Mater. 262, 133-139.

Purova, R., Narasimharao, K., Ahmed, N.S.I., Al-Thabaiti, S., Al-Shehri, A., Mokhtar, M., Schwieger, W., 2015. Pillared HMCM-36 zeolite catalyst for biodiesel production by esterification of palmitic acid. J. Mol. Catal. A Chem. 406, 159-167.

Raia, R.Z., da Silva, L.S., Marcucci, S.M.P., Arroyo, P.A., 2017. Biodiesel production from Jatropha curcas L. oil by simultaneous esterification and transesterification using sulphated zirconia. Catal. Today 289, 105-114.

Rattanaphra, D., Harvey, A.P., Thanapimmetha, A., Srinophakun, P., 2012. Simultaneous transesterification and esterification for biodiesel production with and without a sulphated zirconia catalyst. Fuel 97, 467-475.

Redekop, E.A., Johansson, N., Kokkonen, E., Urpelainen, S., Silva, F.L.d., Kaipio, M., Nieminen, H.-E., Rehman, F., Miikkulainen, V., Ritala, M., Olsbye, U., 2021. Synchronizing gas injections and time-resolved data acquisition for perturbation-enhanced APXPS experiments. Rev. Sci. Instrum. 92, 044101.

Resasco, D.E., Wang, B., Crossley, S., 2016. Zeolite-catalysed C-C bond forming reactions for biomass conversion to fuels and chemicals. Catal. Sci. Technol. 6, 2543-2559.

Resende, R.F., Vieira, S.S., Santos, N.A.V., Fernandes, A., Ribeiro, M.F., Magriotis, Z.M., 2020. Effect of the amount of SO42-/La2O3 on HZSM-5 activity for esterification reaction. Catal. Today 344, 150-157.

Ribeiro, M.E., Franke, K.N., Lima, P.M., Cardoso, D., 2021. Effect of the properties of MFI zeolites on the esterification of isopentyl acetate. Catal. Today 381, 209-214.

Rybicki, M., Sauer, J., 2019. Acid strength of zeolitic Brønsted sites—Dependence on dielectric properties. Catal. Today 323, 86-93.

Sacchetto, V., Bisio, C., Olivas Olivera, D.F., Paul, G., Gatti, G., Braschi, I., Berlier, G., Cossi, M., Marchese, L., 2015. Interactions of Toluene and n-Hexane on High Silica Zeolites: An Experimental and Computational Model Study. J. Phys. Chem. C 119, 24875-24886.

Sánchez-Correa, C.A., Gil-Chaves, I.D., Rodríguez-Niño, G., 2023. Kinetics of acetic acid and isoamyl alcohol liquid esterification over Amberlyst-70. Chem. Eng. Res. Des. 196, 642-655.

Sarazen, M.L., Iglesia, E., 2018. Effects of Charge, Size, and Shape of Transition States, Bound Intermediates, and Confining Voids in Reactions of Alkenes on Solid Acids. ChemCatChem 10, 4028-4037.

Sastre, G., 2016. Confinement effects in methanol to olefins catalysed by zeolites: A computational review. Front. Chem. Sci. Eng. 10, 76-89.

Sastre, G., Corma, A., 2009. The confinement effect in zeolites. J. Mol. Catal. A Chem. 305, 3-7.

Satriadi, H., Pratiwi, I.Y., Khuriyah, M., Widayat, Hadiyanto, Prameswari, J., 2022. Geothermal solid waste derived Ni/Zeolite catalyst for waste cooking oil processing. Chemosphere 286, 131618.

Satyarthi, J.K., Radhakrishnan, S., Srinivas, D., 2011. Factors Influencing the Kinetics of Esterification of Fatty Acids over Solid Acid Catalysts. Energ. Fuels. 25, 4106-4112.

Schwalbe-Koda, D., Gómez-Bombarelli, R., 2023. Generating, Managing, and Mining Big Data in Zeolite Simulations. AI-Guided Design and Property Prediction for Zeolites and Nanoporous Materials, pp. 81-111.

Schwalbe-Koda, D., Kwon, S., Paris, C., Bello-Jurado, E., Jensen, Z., Olivetti, E., Willhammar, T., Corma, A., Román-Leshkov, Y., Moliner, M., Gómez-Bombarelli, R., 2021. A priori control of zeolite phase competition and intergrowth with high-throughput simulations. Science 374, 308-315.

Shamzhy, M., Opanasenko, M., Concepción, P., Martínez, A., 2019. New trends in tailoring active sites in zeolite-based catalysts. Chem. Soc. Rev. 48, 1095-1149.

1351 Shan, J., Wang, Q., Hao, H., Guo, H., 2023. Critical Review on the Synthesis of Levulinate Esters from
1352 Biomass-Based Feedstocks and Their Application. Ind. Eng. Chem. Res. 62, 17135-17147.

1353 Shen, W., 2017. A theoretical study of confinement effect of zeolite on the ethylene dimerization reaction.
1354 Microporous Mesoporous Mater. 247, 136-144.

1355 Shi, H., Wang, Y., Hua, R., 2015a. Acid-catalyzed carboxylic acid esterification and ester hydrolysis
1356 mechanism: acylium ion as a sharing active intermediate via a spontaneous trimolecular reaction based on
1357 density functional theory calculation and supported by electrospray ionization-mass spectrometry. Phys.
1358 Chem. Chem. Phys. 17, 30279-30291.

1359 Shi, J., Wang, Y., Yang, W., Tang, Y., Xie, Z., 2015b. Recent advances of pore system construction in
1360 zeolite-catalyzed chemical industry processes. Chem. Soc. Rev. 44, 8877-8903.

1361 Silva, L.L., Florindo, B.R., Catuzo, G.L., Zapelini, I.W., Cardoso, J.V.S., Luna, F.M.T., Cavalcante, C.L.,
1362 Martins, L., 2022. Investigation of the secondary porosity in ill-crystallized or desilicated ZSM-5 zeolites
1363 and its performance on MTH reaction. Mol. Catal. 529, 112557.

1364 Smirnova, E., Kot, S., Kolpak, E., Shestak, V., 2021. Governmental support and renewable energy
1365 production: A cross-country review. Energy 230, 120903.

1366 Soltani, S., Rashid, U., Al-Resayes, S.I., Nehdi, I.A., 2017. Recent progress in synthesis and surface
1367 functionalization of mesoporous acidic heterogeneous catalysts for esterification of free fatty acid
1368 feedstocks: A review. Energy Convers. Manag. 141, 183-205.

1369 Srinivasan, P.D., Patil, B.S., Zhu, H., Bravo-Suárez, J.J., 2019. Application of modulation excitation-phase
1370 sensitive detection-DRIFTS for in situ/operando characterization of heterogeneous catalysts. React. Chem.
1371 Eng. 4, 862-883.

1372 Sultana, A., Fujitani, T., 2017. Conversion of levulinic acid to BTX over different zeolite catalysts. Catal.
1373 Commun. 88, 26-29.

1374 Sun, P., Wang, H., Huang, J., Ling, W., Liao, Y., Wang, C., 2023. Competitive adsorption of alcohols over
1375 heteroatom zeolites hinders the catalytic conversion of sugar. Appl. Catal. A Gen. 662, 119258.

1376 Tabor, E., Bernauer, M., Wichterlová, B., Dedecek, J., 2019. Enhancement of propene oligomerization and
1377 aromatization by proximate protons in zeolites; FTIR study of the reaction pathway in ZSM-5. Catal. Sci.
1378 Technol. 9, 4262-4275.

Tang, X., Chen, W., Yi, X., Liu, Z., Xiao, Y., Chen, Z., Zheng, A., 2021. In Situ Observation of Non-Classical 2-Norbornyl Cation in Confined Zeolites at Ambient Temperature. Angew. Chem., Int. Ed. 60, 4581-4587.

Tesser, R., Casale, L., Verde, D., Di Serio, M., Santacesaria, E., 2010. Kinetics and modeling of fatty acids esterification on acid exchange resins. Chem. Eng. J. 157, 539-550.

Thiele, E.W., 1939. Relation between Catalytic Activity and Size of Particle. Ind. Eng. Chem. 31, 916-920.

Tian, Y., Zhang, F., Wang, J., Cao, L., Han, Q., 2021. A review on solid acid catalysis for sustainable production of levulinic acid and levulinate esters from biomass derivatives. Bioresource Technol. 342, 125977.

Toledo, M.V., José, C., Suster, C.R.L., Collins, S.E., Portela, R., Bañares, M.A., Briand, L.E., 2021. Catalytic and molecular insights of the esterification of ibuprofen and ketoprofen with glycerol. Mol. Catal. 513, 111811.

Toledo, M.V., Llerena Suster, C.R., Ferreira, M.L., Collins, S.E., Briand, L.E., 2017. Molecular recognition of an acyl–enzyme intermediate on the lipase B from Candida antarctica. Catal. Sci. Technol. 7, 1953-1964.

Trachta, M., Bulánek, R., Bludský, O., Rubeš, M., 2022. Brønsted acidity in zeolites measured by deprotonation energy. Sci. Rep. 12, 7301.

Treps, L., Demaret, C., Wisser, D., Harbuzaru, B., Méthivier, A., Guillon, E., Benedis, D.V., Gomez, A., Bruin, T.d., Rivallan, M., Catita, L., Lesage, A., Chizallet, C., 2021. Spectroscopic Expression of the External Surface Sites of H-ZSM-5. J. Phys. Chem. C 125, 2163-2181.

Umansky, B., Engelhardt, J., Hall, W.K., 1991. On the strength of solid acids. J. Catal. 127, 128-140.

Van der Mynsbrugge, J., Visur, M., Olsbye, U., Beato, P., Bjørgen, M., Van Speybroeck, V., Svelle, S., 2012. Methylation of benzene by methanol: Single-site kinetics over H-ZSM-5 and H-beta zeolite catalysts. J. Catal. 292, 201-212.

Van Speybroeck, V., Bocus, M., Cnudde, P., Vanduyfhuys, L., 2023. Operando Modeling of Zeolite-Catalyzed Reactions Using First-Principles Molecular Dynamics Simulations. ACS Catal. 11455-11493.

Van Speybroeck, V., De Wispelaere, K., Van der Mynsbrugge, J., Vandichel, M., Hemelsoet, K., Waroquier, M., 2014. First principle chemical kinetics in zeolites: the methanol-to-olefin process as a case study. Chem. Soc. Rev. 43, 7326-7357.

1407 Van Speybroeck, V., Hemelsoet, K., Joos, L., Waroquier, M., Bell, R.G., Catlow, C.R.A., 2015. Advances
1408 in theory and their application within the field of zeolite chemistry. Chem. Soc. Rev. 44, 7044-7111.

1409 van Vreeswijk, S.H., Weckhuysen, B.M., 2022. Emerging analytical methods to characterize zeolite-based
1410 materials. Natl. Sci. Rev. 9.

1411 Vayssilov, G.N., Aleksandrov, H.A., Dib, E., Costa, I.M., Nesterenko, N., Mintova, S., 2022. Superacidity
1412 and spectral signatures of hydroxyl groups in zeolites. Microporous Mesoporous Mater. 343, 112144.

1413 Vecchietti, J., Belletti, G., Quaino, P., Bonivardi, A., Collins, S., 2023. Time-resolved DRIFT spectroscopy
1414 study of carbonaceous intermediates during the water gas shift reaction over Au/ceria catalyst.
1415 ChemCatChem 15, e202300435.

1416 Verboekend, D., Pérez-Ramírez, J., 2011. Design of hierarchical zeolite catalysts by desilication. Catal.
1417 Sci. Technol. 1, 879-890.

1418 Vermeiren, W., Gilson, J.-P., 2009. Impact of Zeolites on the Petroleum and Petrochemical Industry. Top.
1419 Catal. 52, 1131-1161.

1420 Vieira, S.S., Magriotis, Z.M., Graça, I., Fernandes, A., Ribeiro, M.F., Lopes, J.M.F.M., Coelho, S.M.,
1421 Santos, N.A.V., Saczk, A.A., 2017. Production of biodiesel using HZSM-5 zeolites modified with citric
1422 acid and SO42−/La2O3. Catal. Today. 279, Part 2, 267-273.

1423 Vieira, S.S., Magriotis, Z.M., Santos, N.A.V., Saczk, A.A., Hori, C.E., Arroyo, P.A., 2013. Biodiesel
1424 production by free fatty acid esterification using lanthanum (La3+) and HZSM-5 based catalysts.
1425 Bioresource Technol. 133, 248-255.

1426 Villoria-del-Álamo, B., Rojas-Buzo, S., García-García, P., Corma, A., 2020. Zr-MOF-808 as Catalyst for
1427 Amide Esterification. Chem. Eur. J. 27, 4588.

1428 Wang, H., Hou, Y., Sun, W., Hu, Q., Xiong, H., Wang, T., Yan, B., Qian, W., 2020. Insight into the Effects
1429 of Water on the Ethene to Aromatics Reaction with HZSM-5. ACS Catal. 10, 5288-5298.

1430 Wei, Y.-S., Zhang, M., Zou, R., Xu, Q., 2020. Metal–Organic Framework-Based Catalysts with Single
1431 Metal Sites. Chem. Rev. 120, 12089-12174.

1432 Weinberg, W.H., 1996. Eley−Rideal Surface Chemistry: Direct Reactivity of Gas Phase Atomic Hydrogen
1433 with Adsorbed Species. Acc. Chem. Res. 29, 479-487.

1434 Weissenberger, T., Machoke, A.G.F., Reiprich, B., Schwieger, W., 2021. Preparation and Potential
1435 Catalytic Applications of Hierarchically Structured Zeolites with Macropores. Adv. Mater. Interfaces 8,
1436 2001653.
1437 Wen, Z., Yang, D., He, X., Li, Y., Zhu, X., 2016. Methylation of benzene with methanol over HZSM-11
1438 and HZSM-5: A density functional theory study. J. Mol. Catal. A Chem. 424, 351-357.
1439 Wu, J., Murphy, B.M., Gould, N.S., Wang, C., Ma, L., Xu, B., 2019. A FTIR Study of the Acidity of in
1440 situ Generated Brønsted Sites on NaY via Displacement Reactions. ChemCatChem 11, 3253-3263.
1441 Xiao, Y., Chen, W., Yi, X., Peng, W., Liu, Z., Xia, H., Zheng, A., 2021. Confinement-Driven "Flexible"
1442 Acidity Properties of Porous Zeolite Catalysts with Varied Probe-Assisted Solid-State NMR Spectroscopy.
1443 J. Phys. Chem. C 125, 11580-11590.
1444 Yan, P., Wang, H., Liao, Y., Wang, C., 2023. Zeolite catalysts for the valorization of biomass into platform
1445 compounds and biochemicals/biofuels: A review. Renew. sustain. energy rev. 178, 113219.
1446 Yang, Y., Xu, R., Zheng, C., Long, Y., Tang, S., Sun, Z., Huang, B., Chen, J.P., 2022. Hierarchical hollow
1447 zeolite fiber in catalytic applications: A critical review. Chemosphere 307, 135899.
1448 Yi, X., Peng, Y.-K., Chen, W., Liu, Z., Zheng, A., 2021. Surface Fingerprinting of Faceted Metal Oxides
1449 and Porous Zeolite Catalysts by Probe-Assisted Solid-State NMR Approaches. Acc. Chem. Res. 54, 2421-
1450 2433.
1451 Yuan, J., Gao, M., Liu, Z., Tang, X., Tian, Y., Ma, G., Ye, M., Zheng, A., 2023. Hyperloop-like diffusion
1452 of long-chain molecules under confinement. Nat. Commun. 14, 1735.
1453 Yuan, Y., Brady, C., Annamalai, L., Lobo, R.F., Xu, B., 2021. Ga speciation in Ga/H-ZSM-5 by in-situ
1454 transmission FTIR spectroscopy. J. Catal. 393, 60-69.
1455 Zalazar, M.F., Cabral, N.D., Romero Ojeda, G.D., Alegre, C.I.A., Peruchena, N.M., 2018a. Confinement
1456 Effects in Protonation Reactions Catalyzed by Zeolites with Large Void Structures. J. Phys. Chem. C.,
1457 27350–27359.
1458 Zalazar, M.F., Paredes, E.N., Romero Ojeda, G.D., Cabral, N.D., Peruchena, N., 2018b. Study of
1459 Confinement and Catalysis Effects of the Reaction of Methylation of Benzene by Methanol in H-Beta and
1460 H-ZSM-5 Zeolites by Topological Analysis of Electron Density. J. Phys. Chem. C. 122, 3350–3362.

1461 Zapelini, I.W., Lorena da Silva, L., Mintova, S., Cardoso, D., 2023. Amine-grafted H-MFI zeolite
1462 precursors as acidic-basic catalysts for deacetalization-Knoevenagel condensation. Microporous
1463 Mesoporous Mater. 362, 112776.

1464 Zhai, D., Liu, Y., Zheng, H., Zhao, L., Gao, J., Xu, C., Shen, B., 2017. A first-principles evaluation of the
1465 stability, accessibility, and strength of Brønsted acid sites in zeolites. J. Catal. 352, 627-637.

1466 Zhang, H., Samsudin, I.b., Jaenicke, S., Chuah, G.-K., 2022. Zeolites in catalysis: sustainable synthesis and
1467 its impact on properties and applications. Catal. Sci. Technol. 12, 6024-6039

1468 Zhang, Q., Gao, S., Yu, J., 2023. Metal Sites in Zeolites: Synthesis, Characterization, and Catalysis. Chem.
1469 Rev. 123, 6039-6106.

1470 Zhang, Q., Yu, J., Corma, A., 2020. Applications of Zeolites to C1 Chemistry: Recent Advances,
1471 Challenges, and Opportunities. Adv. Mater. 32, 2002927.

1472 Zhang, W., Chu, Y., Wei, Y., Yi, X., Xu, S., Huang, J., Zhang, M., Zheng, A., Deng, F., Liu, Z., 2016.
1473 Influences of the confinement effect and acid strength of zeolite on the mechanisms of Methanol-to-Olefins
1474 conversion over H-ZSM-5: A theoretical study of alkenes-based cycle. Microporous Mesoporous Mater.
1475 231, 216-229.

1476 Zholobenko, V., Freitas, C., Jendrlin, M., Bazin, P., Travert, A., Thibault-Starzyk, F., 2020. Probing the
1477 acid sites of zeolites with pyridine: Quantitative AGIR measurements of the molar absorption coefficients.
1478 J. Catal. 385, 52-60.

1479 Zhou, D., Wang, L., Chen, X., Wei, X., Liang, J., Tang, R., Xu, Y., 2020. Reaction mechanism investigation
1480 on the esterification of rosin with glycerol over annealed Fe3O4/MOF-5 via kinetics and TGA-FTIR
1481 analysis. Chem. Eng. J. 401, 126024.

1482

Highlights

- Zeolites can be used as remediation tools for the recovery of oily wastes.
- Unraveling Esterification on H-Zeolites: Experimental and theoretical Insights.
- Esterification yields for FFAs can be improved by knowing the reaction mechanism.
- Advanced MES-PSD spectroscopy techniques are presented in catalytic processes.

.

Declaration of interests

☒ The authors declare that they have no known competing financial interests or personal relationships that could have appeared to influence the work reported in this paper.

☐The authors declare the following financial interests/personal relationships which may be considered as potential competing interests: